12-2019

Portable Electrochemical System for Flexible Hybrid Electronics

Anthony Joseph Hanson
Western Michigan University

PORTABLE ELECTROCHEMICAL SYSTEM FOR FLEXIBLE HYBRID ELECTRONICS

by

Anthony Joseph Hanson

A thesis submitted to the Graduate College
in partial fulfillment of the requirements
for the degree of Master of Science in Engineering
Electrical and Computer Engineering
Western Michigan University
December 2019

Thesis Committee:

Massood Z. Atashbar, Ph.D.,
Chair Bradley J. Bazuin, Ph.D.
Binu B. Narakathu, Ph.D.

ACKNOWLEDGMENTS

First, I would like to thank my graduate advisor and committee chair Dr. Massood Atashbar. Thank you for all the opportunities you have given me over the course of my time knowing you. When I started working with you in fall 2017, I knew very little about the FHE industry but thanks to your help that has changed. I've felt you've always believed I would make for a good engineer, and that has pushed me to always try my best. Thank you for constantly find opportunities for me that will both benefit my knowledge and life. You always encouraging me to try new projects and let me research and develop projects I am interested in. I am truly grateful for the impact you have on my life.

Thank you, Dr. Binu Narakathu for all the advice you give me! You have always respected my ideas on projects and encourage me to be creative and think outside the box. You believe in my abilities and I hope to keep proving them to you in years to come.

Also, thank you Dr. Bradley Bazuin for teaching me skills that will further enhance my engineer passion. I've learned from you that there are a lot of ways to complete a task but finding the best way (even if it is challenging) is what makes a great engineer.

I would also like to thank my family for supporting me and pushing me to do my best. Lastly, thank you to all the members in the Center for Advanced Smart Sensors and Structures (CASSS), they help me every day no matter the task and I am truly appreciative of that.

Anthony Hanson

PORTABLE ELECTROCHEMICAL SYSTEM FOR FLEXIBLE HYBRID ELECTRONICS

Anthony Joseph Hanson, M.S.E.

Western Michigan University, 2019

This work focuses on the fabrication and design of a portable electrochemical sensing system for flexible hybrid electronic (FHE) sensors. A three-electrode chemical sensor was fabricated using copper tape on polyethylene terephthalate (PET) substrate, using laser etching process. An electronic circuit was designed to measure the sensor response through electrochemical techniques to detect different concentrations of glucose. The device was calibrated to give the user a concentration value in 5 seconds. The system was also designed to preform tests such as cyclic voltammogram and chronoamperogram for various chemicals. A Bluetooth Low Energy module was used to wirelessly transmit the results to a smart phone for post analysis. The system was powered with a 3.7V lithium polymer battery using an average of 2.8 mA during the test.

TABLE OF CONTENTS

LIST OF TABLES

LIST OF FIGURES

CHAPTER 1
INTRODUCTION

1.1 Background

For the past decade, there has been lots of time, money, and research that has gone into making electronics thin and light weight while making them relatively cost-efficient [1]. The result of this interest has shined a light on flexible hybrid electronics, also known as FHE. FHE allows electronic systems to be used in applications where traditional electronics cannot function. FHE brings many more benefits such as roll-to-roll manufacturing, time-to-market, and reduced manufacturing cost all while being on a conformable substrate [2]. With this technology, a door has opened to make sensors thin and flexible. A variety of sensors like strain, pressure, temperature, humidity, touch, proximity, and chemical have been fabricated using FHE methods [3-53]. These sensors which are fabricated on thin, flexible substrates in large volume gives industrial companies an enormous option for new applications where sensors have not been used before [54].

With bio-sensing being a major need in the electronics industry, sensors for monitoring strain, temperature, ECG, and bio-chemicals have great potential for wearable applications [55]. Chemical sensors have been proven to work for sensing the concentrations of various materials. Some chemicals that can be found in the biological species are potassium chloride, cadmium saline, and glucose [56]. Others can be heavy metals like lead nitrate and cadmium nitrate [57-58]. Sensing chemicals usually involves stationary, bulky and expensive lab equipment to get an accurate reading of the concentration. With all the recent research of making printed chemical sensors on

various substrates and providing roll-to-roll manufacturing, a large piece of lab equipment is still necessary to read the sensors. This leads to the need of a portable, all-in-one system which can do the same important functions as the larger lab-based equipment.

1.2 Thesis Organization

The contents of this thesis are organized into four chapters. In Chapter 2, a background of FHE will be discussed which will include fabrication techniques, types of FHE sensors, and applications where these sensors can be used. Chapter 2 will also discuss chemical sensing methods and electrochemical sensor designs. Chapter 3 will focus on the development of the system including the sensor design and fabrication, hardware used in the electronic readout, and the software used to calibrate the device. This chapter will also include the results from the system. Finally, Chapter 4 will summarize the present work and provide suggestions to further improve the system.

1.3 References

[1] A. Kamyshny, S. Magdassi, “Conductive Nanomaterials for Printed Electronics”, Small, vol. 10(17), pp.3515-3535, 2014.

[2] T. Huang, L. Shao, T. Lei, R. Beausoleil, Z. Bao, K. Cheng, "Robust design and design automation for flexible hybrid electronics," 2017 IEEE International Symposium on Circuits and Systems (ISCAS), pp. 1-4, 2017.

[3] A. S. G. Reddy, B. B. Narakathu, M. Z. Atashbar, M. Rebros, E. Rebrosova, and M. K. Joyce, “Fully printed flexible humidity sensor”, Procedia Engineering, vol. 25, pp. 120-123, 2011.

[4] M. Z. Atashbar, M. M. Ali, B. B. Narakathu, and A. Eshkeiti, “Metal-metal composite ink and methods for forming conductive patterns”, U.S. Patent Application No. 15/827,312, 2018.

[5] A.S.G. Reddy, B.B. Narakathu, M.Z. Atashbar, M. Rebros, E. Rebrosova, M.K. Joyce, “Gravure Printed Electrochemical Biosensors”, 25th Eurosensors Conference, September 4 – 7, 2011, Athens, vol. 25, pp. 956-959, 2011.

[6] A. Eshkeiti, S. Emamian, A. S. G. Avathu, B. B. Narakathu, M. J. Joyce, M. K. Joyce, M. Z. Atashbar, “Screen printed flexible capacitive pressure sensor.”, In SENSORS IEEE, pp. 1192-1195, 2014

[7] S.G.R. Reddy, B.B. Narakathu, M.Z. Atashbar, M. Rebros, E. Hrehorova, B.J. Bazuin, M.K. Joyce, P.D. Fleming, A. Pekarovicova, “Printed capacitive based humidity sensors on flexible substrates”, Sensor Letters, vol. 9, pp. 869-871, 2011.

[8] S.G.R. Avuthu, B.B. Narakathu, M.Z. Atashbar, M. Rebros, E Hrehorova, B. Bazuin, D. Fleming, M. Joyce “Printed Capacitive Based Humidity Sensors on Flexible Substrates” 13th International Meeting on Chemical Sensors, July 11-14, 2010, Perth, Australia, pp. 124, 2010.

[9] D. Alsaid, E. Rebrosova, M. Joyce, M. Rebros, M.Z. Atashbar, B. Bazuin “Gravure Printing of ITO Transparent Electrodes for Applications in Flexible

Electronics” IEEE Journal of Display Technology, vol. 8, No. 7, pp. 391-396, 2012.

[10] V.N. Bliznyuk, S. Singamaneni, R. Kattumenu, M.Z. Atashbar “Surface electrical conductivity in ultrathin single-wall carbon nanotube/polymer nanocomposite films” Applied Physics Letters, 88, pp. 164101-164103, 2006.

[11] B.B. Narakathu, M.S. Devadas, A. S. G. Reddy, A. Eshkeiti, A. Moorthi, I.R. Fernando, B. Miller, G. Ramakrishna, E. Sinn, M. Joyce, M. Rebros, E. Rebrosova, G. Mezei and M.Z. Atashbar, “Novel Fully Screen Printed Flexible Electrochemical Sensor for the Investigation of Electron Transfer between Thiol Functionalized Viologen and Gold Clusters”, Sensors and Actuators B: Chemical, vol. 176, pp. 768-774, 2012.

[12] A.S.G. Reddy, B.B. Narakathu, M.Z. Atashbar, M. Rebros, E. Hrehorova, M. Joyce, “Printed electrochemical based biosensors on flexible substrates” IEEE Sensors Conference, November 1-4, 2010, Waikoloa, HI, USA, pp. 1596-1600, 2010.

[13] B.B. Narakathu, W. Guo, S.O. Obare, M.Z. Atashbar “Electrochemical Impedance Spectroscopy Sensing of Toxic Organophosphorus Compounds” IEEE Sensors Conference, November 1-4, 2010, Waikoloa, HI, USA. Pp. 1518-1521, 2010.

[14] D. Go, M.Z. Atashbar, Z. Ramshani, and H.C. Chan “Surface acoustic wave devices for chemical sensing and microfluidics: A review and perspective” Analytical Methods, 9, 4112-4134, 2017, DOI: 10.1039/C7AY00690J

[15] B. Ziaie, A. Baldi, M.Z. Atashbar “Introduction to micro/nanofabrication” in Nanotechnology Handbook, B. Bhushan, ed., Springer-Verlag, Heidelberg, Germany, pp. 147-184, first edition, 2004; Second Edition, pp. 197-237, 2007; pp. 231-269, Third Edition, 2010, pp.51-86 Fourth Edition 2017.

[16] S. Emamian, A. Eshkeiti, A. S. G. Reddy, B. B. Narakathu, M. Z. Atashbar, “Gravure printed flexible surface enhanced Raman spectroscopy (SERS) substrate for detection of 2,4-dinitrotoluene (DNT) vapor”, Sensors and Actuators B: Chemical, vol. 217(1), pp. 129-135, 2014.

[17] M.Z. Atashbar and S. Singamaneni “Comparative studies of temperature dependence of ‘G’ band peak in SWNT and highly oriented pyrolytic graphite” Applied physics Letters, 86, pp. 123112-1 to 123112-3, 2005.

[18] V. S. Turkani, D. Maddipatla, B. B. Narakathu, B. J. Bazuin, M. Z. Atashbar, “A Fully Printed CNT Based Humidity Sensor on Flexible PET Substrate”, 17th International Meeting on Chemical Sensors (IMCS), July 15-19, Vienna, Austria, pp. 519-520, 2018

[19] M.Z. Atashbar, B.J. Bazuin, M. Simpeh, S. Krishnamurthy “3-D finite-element simulation model of SAW palladium thin film hydrogen sensor” 2004 IEEE International Ultrasonics, Ferroelectrics, and Frequency Control, August 23-27 2004 pp. 549-553, Monntreal, Canada, 2004.

[20] M Z. Atashbar, A. A. Chlaihawi, B. B. Narakathu, and A. Eshkeiti, “Printed ecg electrode and method”, U.S. Patent Application No. 15/591,856, 2017

[21] B.B. Narakathu, A. Eshkeiti, A.S.G. Reddy, A. Moorthi, M.Z. Atashbar, “A Novel Fully Printed and Flexible Capacitive Pressure Sensor”, 11th IEEE Sensors Conference, October 28-31, 2012, Taipei, Taiwan, pp. 1935-1938.

[22] M.Z. Atashbar, B. Bejcek S. Singamaneni “Carbon nanotube-network based biomolecule detection” IEEE Sensors Journal, 6, 3, pp. 524- 528, 2006.

[23] B.B. Narakathu, W. Guo, S.O. Obare, M.Z. Atashbar, “Novel approach for detection of toxic organophosphorus compounds”, Sensors and Actuators B: Chemical, vol. 158, pp. 69-74, 2011.

[24] A.A. Chlaihawi, S. Emamian, B.B. Narakathu, M.M. Ali, D. Maddipatla, B. J. Bazuin, M. Z. Atashbar. "A screen printed and flexible piezoelectric-based AC magnetic field sensor." Sensors and Actuators A: Physical 268 (2017): 1-8.

[25] V. Palaniappan, et.al. “Laser-Assisted Fabrication of Flexible Micro-Structured Pressure Sensor for Low Pressure Applications” 2019 IEEE International Conference on Flexible and Printable Sensors and Systems (FLEPS), pp. 1-3, 2019. DOI: 10.1109/FLEPS.2019.8792235.

[26] M.Z. Atashbar, B. Bejcek, S. Singamaneni “Carbon nanotube based biosensors” IEEE Sensor conference, Vienna, Austria, Oct. 24th-27th, 2004, pp. 1048 – 1051, 2004.

[27] S. Lim, M. Joyce, P. D. Fleming, A.T. Aijazi, M.Z. Atashbar, “Inkjet Printing and Sintering of Nano copper ink” Journal of Imaging Science and Technology, Vol 57, No. 5, pp. 50506-1-50506-7, 7, 2013.

[28] Z. Ramshani, A.S.G. Reddy, B.B. Narakathu, M.Z. Atashbar, “SH-SAW sensor based microfluidic system for the detection of heavy metal compounds in liquid environments”, Sensors and Actuators B: Chemical, vol. 217, 1, pp. 72-77, 2015.

[29] V. S . Turkani,D. Maddipatla, B.B. Narakathu, B.J. Bazuin, and M.Z. Atashbar, “A Carbon Nanotube Based NTC Thermistor using Additive Print Manufacturing Processes” Sensors and Actuators A: Physical. 279, 15, 1-9, 2018, https://doi.org/10.1016/j.sna.2018.05.042

[30] N. Ghafouri, H. Kim, M.Z. Atashbar, K. Najafi “A microscale thermoelectric energy scavenger for a hybrid insect” The 7th IEEE Conference on Sensors October 26-29, 2008, Lecce, Italy, pp. 1249-1252, 2008.

[31] D. Maddipatla, B.B. Narakathu, S.G.R. Avuthu, S. Emamian, A. Eshkeiti, A.A. Chlaihawi, B.J. Bazuin, M.K. Joyce, C.W. Barrett, M.Z. Atashbar, “A novel flexographic printed strain gauge on paper platform”, 14th IEEE Sensors Conference, November 1-4, Busan, South Korea, pp. 1657-1660, 2015.

[32] D. Maddipatla, BB Narakathu, M.M. Ali, AA Chlaihawi, M.Z. Atashbar “Development of a novel carbon nanotube based printed and flexible pressure sensor, IEEE Sensors Applications Symposium, SAS, pp. 1-4, 2017.

[33] B.B. Narakathu, A.S.G. Reddy, A. Eshkeiti, S. Emamian, M.Z. Atashbar, “Development of a microfluidic sensing platform by integrating PCB technology and inkjet printing process”, IEEE Sensors Journal, vol. 15, 11, pp. 6374 - 6380, 2015.

[34] M.K. Joyce, M.J. Joyce, A. Eshkeiti, M.Z. Atashbar, P. D. Fleming “Self-supported electronic devices” United States Patent Publication US WO2016019223 A1, February 4, 2016, US Patent App. 15/329,151.

[35] S.G.R. Avuthu, J.T. Wabeke, B.B. Narakathu, D. Maddipatla, J. Arachchilage, S.O Obare, M.Z. Atashbar, “A screen printed phenanthroline based flexible electrochemical sensor for selective detection of toxic heavy metal ions”, pp. 8678 - 8684 IEEE Sensors Journal, 2016. DOI: 10.1109/JSEN.2016.2572184.

[36] M. Ochoa, R. Rahimi, J. Zhou, H. Jiang, C.K. Yoon, M. Oscai, V. Jain, T. Morken, R.H. Oliveira, D. Maddiplata, B.B. Narakathu, G.L. Campana, M.A. Zieger, R. Sood, M.Z. Atashbar, B. Ziaie “A manufacturable smart dressing with oxygen delivery and sensing capability for chronic wound management” Micro-and Nanotechnology Sensors, Systems, and Applications X. Vol. 10639, 106391C, International Society for Optics and Photonics, 2018.

[37] A.A. Chlaihawi, B.B. Narakathu, S. Emamian, B.J. Bazuin, and M.Z. Atashbar, “Development of printed and flexible dry ECG electrodes” Sensing and Bio-Sensing Research, 20, 9-15, 2018, https://doi.org/10.1016/j.sbsr.2018.05.001

[38] M.M. Ali, D. Maddipatla, B.B Narakathu, A.A. Chlaihawi, S. Emamian, F. Janabi, B.J. Bazuin, M.Z. Atashbar “Printed Strain on silver nanowire/silver flake composite on flexible and stretchable TPU substrate” Sensors and Actuators A: Physical, 274, 109-115, 2018 https://doi.org/10.1016/j.sna.2018.03.003

[39] S. Emamian, B.B. Narakathu, A. Chlaihawi, B. Bazuin, and M.Z. Atashbar “Screen Printing of Flexible Piezoelectric Based Device on Polyethylene Terephthalate, PET and Paper for Touch and Force Sensing Applications”

journal Sensors & Actuators: A. Physical, 263, 639-647, 2017. https://doi.org/10.1016/j.sna.2017.07.045

[40] S. Emamian, S.G.R. Avuthu, B.B. Narakathu, A. Eshkeiti, A.A. Chlaihawi, B.J. Bazuin, M.Z. Atashbar, “Fully printed and flexible piezoelectric based touch sensitive skin”, 14th IEEE Sensors Conference, November 1-4, Busan, South Korea, pp. 1827-1830, 2015.

[41] A.A. Chlaihawi, S. Emamian, B.B Narakathu, M.M Ali, D. Maddipatla, B.J. Bazuin, and M.Z. Atashbar, “A Screen Printed and Flexible Piezoelectric Based AC Magnetic Field Sensor” Sensors and Actuators, 268, 1-8, 2017. https://doi.org/10.1016/j.sna.2017.10.030

[42] M.M. Ali, B.B. Narakathu, S. Emamian, A.A. Chlaihawi, F. Aljanabi, D. Maddipatla, B.J. Bazuin, M.Z. Atashbar, “Eutectic Ga-In liquid metal based flexible capacitive pressure sensor”, 15th IEEE Sensors Conference, October 30 – November 2, Orlando, Florida, USA, pp. 352-354, 2016.

[43] M.M. Ali, B.B. Narakathu, S. Emamian, A.A. Chlaihawi, F. Aljanabi, D. Maddipatla, B.J. Bazuin, M.Z. Atashbar, “Eutectic Ga-In liquid metal based flexible capacitive pressure sensor”, 15th IEEE Sensors Conference, October 30 – November 2, Orlando, Florida, USA, pp. 352-354, 2016.

[44] A.A. Chlaihawi, B.B. Narakathu, A. Eshkeiti, S. Emamian, A.S.G. Reddy, M.Z. Atashbar, “Screen printed MWCNT/PDMS based dry electrode sensor for electrocardiogram, ECG measurements”, IEEE International Conference on Electro/Information Technology, EIT, May 21-23, Dekalb, Illinois, USA, pp. 526-529, 2015.

[45] A. Eshkeiti, M.J. Joyce, B.B. Narakathu, S. Emamian, S.G.R. Avuthu, M. Joyce, M.Z. Atashbar, “A Novel Self-Supported Printed Flexible Strain Sensor for Monitoring Body Movement”, 13th IEEE Sensors Conference, November 2-5, 2014, Valencia, Spain, pp.1069-1072.

[46] B. N. Altay, J. Jourdan, H. Dietsch, V.S. Turkani, D. Maddipatla, A. Pekarovicova, P. D. Fleming, M.Z. Atashbar “Impact of substrate and process on the electrical performance of screen-printed nickel electrodes: fundamental mechanism of ink film roughness” ACS Applied Energy Materials, ACS Applied Energy Materials 1 (12), 7164-7173, 2018. DOI: 10.1021/acsaem.8b0161

[47] D. Maddipatla, Farah Janabi, B. Narakathu1, S. Ali, B. Bazuin, D. Fleming, M.Z. Atashbar “Development of a novel wrinkle-structure based SERS substrate for drug detection applications” Sensing and Bio-Sensing Research Volume 24, 100281, June 2019. https://doi.org/10.1016/j.sbsr.2019.100281

[48] D. Maddipatla, B.B Narakathu,M. Ochoa, R. Rahimi, J. Zhou, C. Yoon, J. H. Chang; H. Al-Zubaidi, S. Obare, M. Zieger, B. Ziaie, M.Z. Atashbar “Rapid prototyping of a novel and flexible paper based oxygen sensing patch via additive inkjet printing process", RSC Adv., 9, 22695-22704, 2019, DOI: 10.1039/C9RA02883H.

[49] V.S. Turkani, D. Maddipatla, B.B. Narakathu, T.H.S. Saeed, S.O. Obare, B.J. Bazuin, and M.Z. Atashbar “A Highly Sensitive Printed Humidity Sensor based on Functionalized MWCNT/HEC Composite for Flexible Electronics Application” Nanoscale Advances, 1, 2311-2322, 2019, DOI: 10.1039/C9NA00179D

[50] B.B. Narakathu, B.E. Bejcek and M.Z. Atashbar, “Pico mole level detection of toxic biochemical species using impedance based electrochemical biosensors”, Sensor Letters, vol. 9, pp. 872-875, 2011.

[51] V.S. Turkani, D. Maddipatla, B.B. Narakathu, B.N. Altay, P.D. Fleming, B.J. Bazuin, and M.Z. Atashbar “Printed Nickel based RTD on Flexible Polyimide Substrate” IEEE ACESS, 2019, DOI: 10.1109/ACCESS.2017

[52] B. B. Narakathu, B. E. Bejcek and M. Z. Atashbar, "Impedance based electrochemical biosensors," IEEE SENSORS, pp. 1212-1216, 2009.

[53] S.G.R Avuthu et.al , "Detection of heavy metals using fully printed three electrode electrochemical sensor," IEEE SENSORS, pp. 669-672, 2014.

[54] M. Mashayekhi, "Evaluation of Aerosol, Superfine Inkjet, and Photolithography Printing Techniques for Metallization of Application Specific Printed Electronic Circuits," IEEE Transactions on Electron Devices, vol. 63(3), pp. 1246-1253, 2016.

[55] L. Xie, G. Yang, M. Mäntysalo, F. Jonsson, L. Zheng, "A system-on-chip and paper-based inkjet printed electrodes for a hybrid wearable bio-sensing system," 2012 Annual International Conference of the IEEE Engineering in Medicine and Biology Society, pp. 5026-5029, 2012.

[56] B. B. Narakathu, B. E. Bejcek and M. Z. Atashbar, "Impedance based electrochemical biosensors," IEEE SENSORS, pp. 1212-1216, 2009.

[57] S. Avuthu et.al , "Detection of heavy metals using fully printed three electrode electrochemical sensor," IEEE SENSORS, pp. 669-672, 2014.

[58] S.G.R. Avuthu, J.T. Wabeke, B.B. Narakathu, D. Maddipatla, J.S. Arachchilage, S.O. Obare, M.Z. Atashbar “A screen printed phenanthroline-based flexible electrochemical sensor for selective detection of toxic heavy metal ions”. IEEE Sensors Journal, 16(24):8678-84, 2016.

CHAPTER 2

FLEXIBLE HYBRID ELECTRONICS AND CHEMICAL SENSING

2.1 Introduction

There is a need for electronics to become smaller, faster, and cheaper [1]. FHE can be the solution to making them smaller and cheaper. FHE can redesign the concept of how sensors, electronic components and printed circuit boards are made and used in the industry. An active application in the field right now is biosensing. Biosensing can include reading internal vital signs like heart rate or external parameters like the temperature of the human body. Biosensing applications can also have the need to know chemical concentrations in the body, like glucose levels. This brings the need to integrate chemical sensors into an FHE system. This chapter will give a background on FHE and chemical sensing that already exists.

2.2 Flexible Hybrid Electronics

Traditional electronics are manufactured through a multi-staged process which requires photolithography, vacuum deposition, and electroless plating [2]. This process can lead to a large amount of wasted materials causing this process to be expensive and non-environmentally friendly. Therefore, with FHE the possibility that a printing press can deliver electronics with quick turnaround times compared to traditional methods, while being relatively inexpensive and flexible enough to be placed in locations where electronics have not been used previously is an added advantage [3]. FHE can be advertised as ‘Electronics everywhere – big opportunities’ [3].

2.2.1 Fabrication Techniques

To fabricate FHE, there are five main fabrication techniques that are being used which include screen printing, gravure printing, flexography printing, inkjet printing, and laser etching. These methods all differ from each other in terms of the resolution they produce to viscosity of the material being used. Table 2.1 shows the specifications for the four ink-based fabrication techniques.

Table 2.1. Specification of ink-based fabrication techniques [4].

Techniques	Image Carrier	Resolution (um)	Ink film Thickness (um)	Printing Speed (m/min)	Line Width (um)	Viscosity (Pa.s)
Gravure	Engraved Cylinder	15	0.02-12	8-100	15	0.01-1.1
Flexography	Photopolymer Plate	20	0.17-8	5-180	15	0.01-0.5
Inkjet	Digital	20	0.01-0.5	0.02-5	20	0.001-0.1
Screen	Stencil	50	3-30	0.6-100	30	0.5-50

Of the four ink-based printers, screen printing is the only one that can handle higher viscosity inks. A screen printer uses a squeegee to push the material through a mask onto a substrate (Fig. 2.1). The mask or screen acts as a stencil which creates the design.

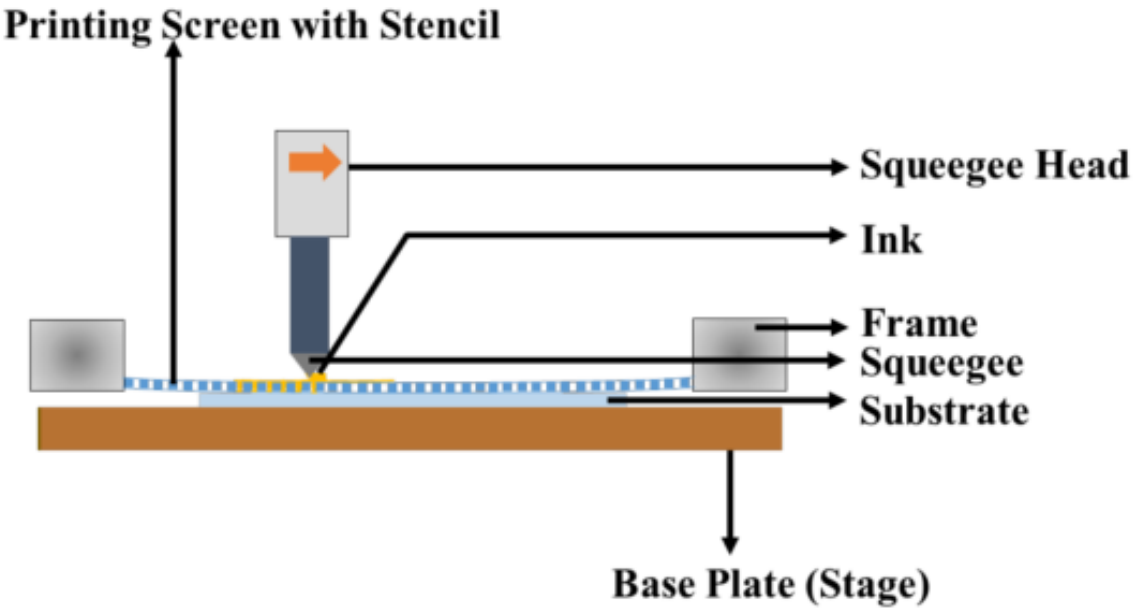

Figure 2.1. Screen printing process [5].

Gravure printing provides the highest resolution of the four ink-based fabrication techniques. This method uses an engraved cylinder which contains the desired design (Fig. 2.2). This system uses a pool of ink under the gravure cylinder. The gravure cylinder grabs the ink and transfers it to the substrate.

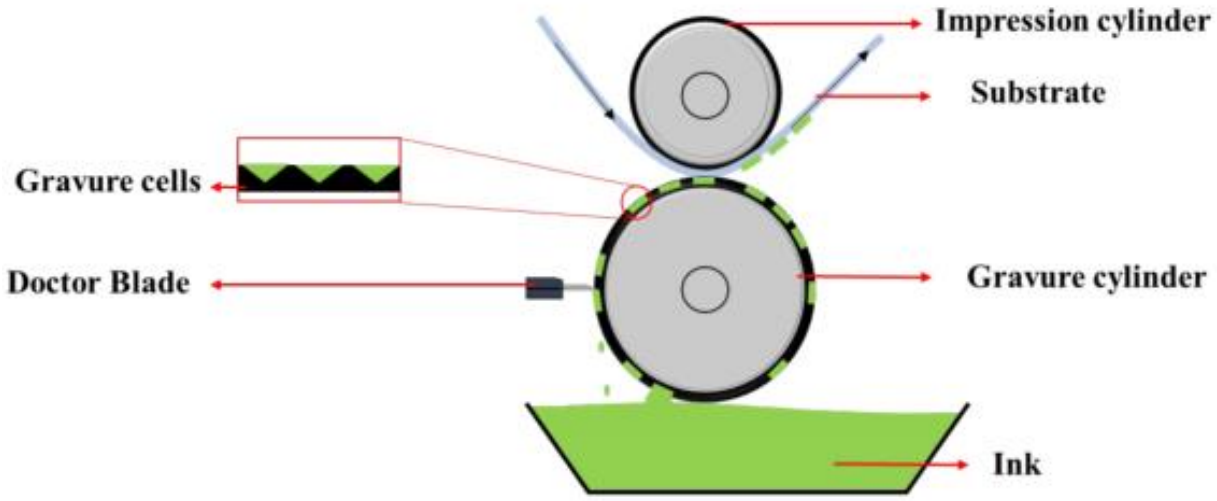

Figure 2.2. Gravure printing process [5].

Flexography printing has the fastest print speed which is useful for large-scale production of FHE. Flexography printing also has the design on a cylinder called the plate cylinder (Fig. 2.3). An anilox roller gets the ink from a reservoir and transfers it onto a plated cylinder. An impression cylinder, under the substrate helps with the transfer process and moving the substrate.

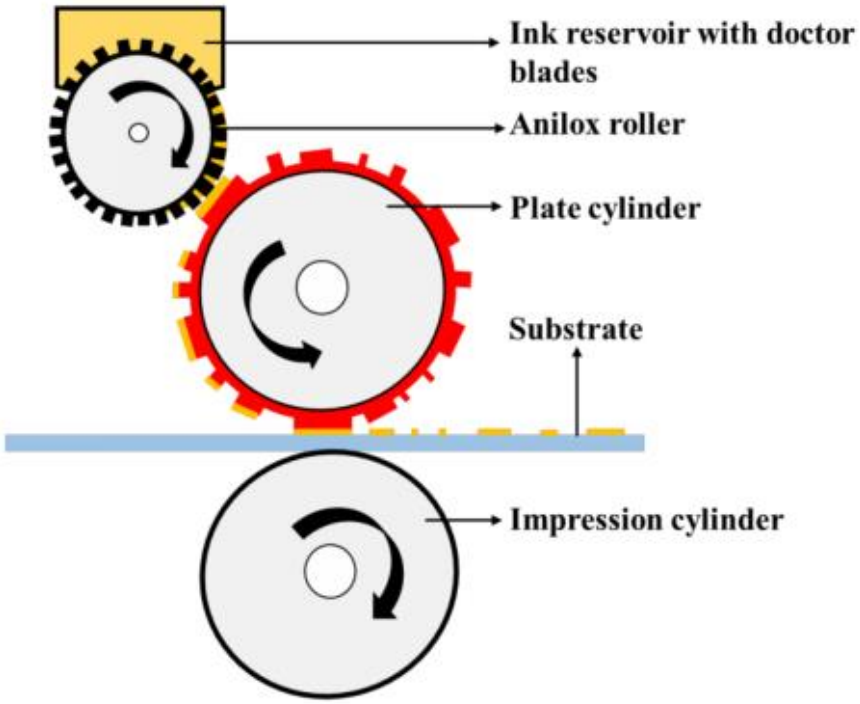

Figure 2.3. Flexography printing process [5].

Inkjet printing is a digital system. The design is contained on a CAD file. This printer moves its nozzle to the areas specified in the design and then extrudes ink onto the substrate (Fig. 2.4). Inkjet printing has a slow printing speed but can print low viscosity inks. This printing method is mainly used for research and development applications because there is no cost when changing the design of a system and can be time effective depending on the change.

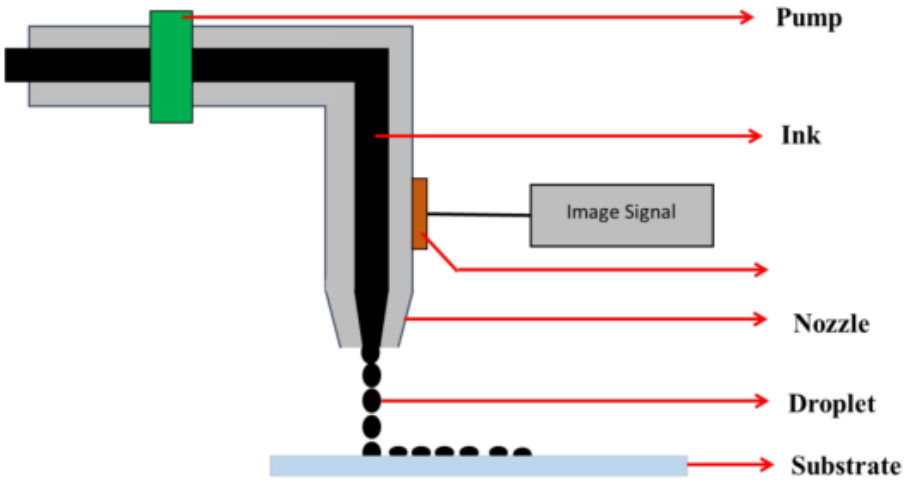

Figure 2.4. Inkjet printing process [5].

Laser etching involves no ink like the other techniques mentioned. This process usually uses a conductive material like copper tape and cuts off the undesired parts (Fig. 2.5). The design is in a CAD file like inkjet printing, so it is relatively easy to change designs. This system can also be used to cut substrates or dielectrics into different designs. The laser head can also be used to carbonize a polymer such as Kapton tape to provide conductive traces using no ink.

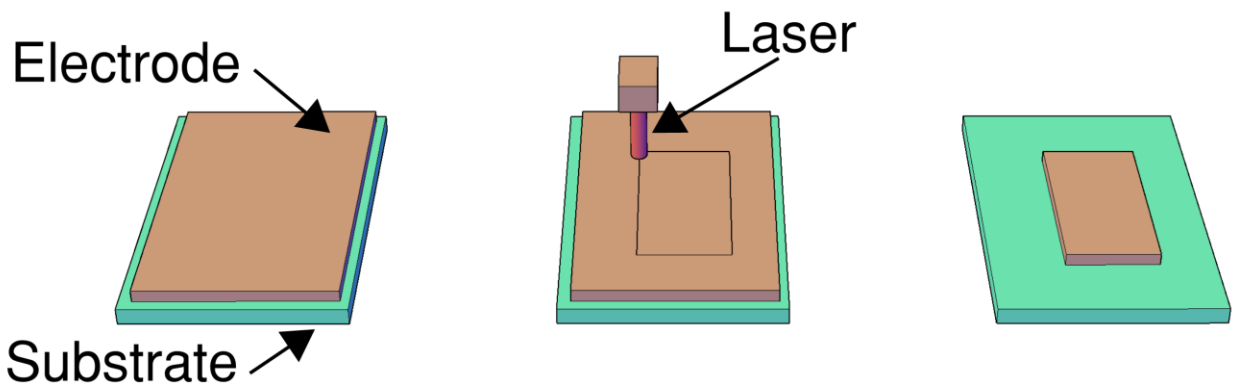

Figure 2.5. Laser etching process.

2.2.2 Sensors

Recently, sensors are being placed all over new and old products. For example, cars that are being made today have a variety of sensors placed in them. This can include blind spot detectors, collision avoidance, and even sensors to determine if a passenger is large enough for the airbags [6]. FHE will play a huge role in further enhancing these sensors. Currently, FHE has been incorporated into some industrial used sensors. A few include humidity, temperature, chemical, pressure, strain, UV, and touch sensors [7-12]. To gather the readings from these sensors, there is a handful of approaches depending on how the sensor was made. A few of the readout methods

used include capacitance, resistance, optical, and frequency. Every sensor will have different parameters - for example, sensitivity, accuracy, or repeatability. These parameters can usually be changed depending on the applications.

2.2.3 Applications for Flexible Hybrid Electronics

As mentioned previously, FHE has a large potential of applications. Robotics for example is a growing industry that can include FHE. Applying a force sensor and temperature sensor to a finger of a robotic hand would provide a feedback to the system indicating how hard the grip being applied is and if the object is warm or not [13]. Strain sensors could also be applied to robotic joints to send feedback on the angle of the joints [14]. This would allow for more accurate and precise movements.

Putting FHE into existing products to make them “smart” is a trend happening in the industry right now. For example, football helmets have changed over the years by developing new materials for the padding and placing the pads in new locations where studies have showed higher chance of injury. Adding FHE into the helmet is a great application because of their light and thin profile. Pressure sensors made using FHE methods could detect where impacts occur and the intensity of an impact without altering the design of the helmet [15]. This information can be valuable for coaches, players, parents, and even the manufacture of the helmets. Thin pressure sensors can also be implemented into other products like socks [16]. This could help with the posture for peoples walking and running while not feeling a difference in their socks.

Renewable energy is also a hot topic right now, and FHE can be implemented for this application too. Energy harvesting systems using piezoelectric materials can be

fabricated with FHE techniques [17]. With a light tap of a pencil, enough energy can be generated to turn on an LED [18]. This technology combined with FHE could replace floor tiles in crowded areas or even strips in road without being noticed and harvesting the energy used every day.

Chemical sensing can provide a wide variety of applications. From finding metals in water [19] to monitoring yeast cell concentration in a miniaturized cell assay [20] to even finding the concentration of glucose in a drop of blood [21]. Most chemical sensors are for single use, so one of the main problems is the cost of each sensor. With FHE being able to fabricate sensors in large scale roll-to-roll manufacturing would make the cost of each sensor relatively cost efficient. This means that these chemical sensors could be used once for an application and then replaced with a new one while keeping maintaining repeatability. For chemical sensing applications, one of the draw backs is the piece of equipment used to monitor the concentration of the desired chemical. There are machines like the PARSTAT 2273 by Ametek to read the response of these sensor using electrochemical methods, but this machine is expensive, bulky, and stationary. For some applications, this defeats the purpose of having a chemical sensor that is fabricated using FHE methods. As stated, some of the advantages to FHE is to make electronics more cost effective and portable, however with needing to attach the sensor to a large instrumentation defeats the purpose. The solution is to make a portable chemical sensing system for FHE.

2.3 Chemical Sensing

With toxic chemicals getting in our water, food, and human body, there is a great need for devices that can indicate its presence and quantity. To do this, the devices use chemical sensors that are designed and calibrated for a certain chemical [22-28]. These devices are being used to detect if the water is safe to drink, and in some places, this device can save lives. Chemical sensors can also be used to indicate if a surface is sterile by detecting the presence of bacteria. Many houses are currently equipped with a carbon monoxide detector which use chemical sensors. The human body is full of chemicals and with a blood test, we can know precisely know the quantity of a certain chemical compound. For example, diabetes which around seven million people develop annually can have a large impact on a person's body [29]. Currently there is no way to cure diabetes, but there is a way to monitor the glucose in the human body thereby improving treatment efficiency [29]. The need to monitor the chemicals is a very important concern in our lives. With this being an important topic for research, in the years ahead we will see these systems being placed in more applications and sensing even more chemicals.

2.3.1 Acquisition Methods

Measuring the response of sensors can be a difficult but an important task. For chemical sensors, there are many methods to read the response of the sensor. One acquisition method is colorimetric based, where the color of the sensor will change. This method is used in pH strips testing strips to determine the pH level of a substance. Using colorimetry, a variety of chemicals can be detected like leukocyte, nitrite, urobilinogen, protein, pH, hemoglobin, specific gravity, ketone, bilirubin, and glucose

[30]. Using a smartphone's camera and a machine-vision algorithm, the program will look at each of the colorimetric squares each relating to a different chemical and detect if the chemical is present and for some, determine the intensity [30]. Optical emission spectroscopy is an acquisition method that has also been used for chemical sensing. Using an optical probe connected to a spectrometer to sweep the wavelength, a micro plasma discharge device can be used to detect which chemicals are present depending on the intensity at specific wave lengths [31]. This acquisition method can be used to detect concentrations as low as 1 pM of lead nitrate or potassium chloride [31].

Another way to read chemical sensors is using the electrochemical sensing method. Electrochemical sensing has been proven to work for biosensing applications because of its ability to sense a variety of chemical compounds and to determine their concentration [32]. With electrochemical sensing, there are three different acquisition methods that can be used: potentiometry, coulometry, or voltammetry. Potentiometry measures the potential voltage between two electrodes, while with coulometry the current throughout the cell is measured and when using voltammetry, current is measured while varying the cell's potential [33]. The author is focusing on the use of voltammetry method which can be used to gather information from cyclic voltammetry graphs as well as chronoamperometry graphs.

2.3.2 Electrochemical Sensor Designs

The electrochemical sensors design can be implemented with a two, three, or four electrode system. In a two-electrode system, the counter and working electrode are used to measure the voltage drop across a system [34]. With the three-electrode design, a reference electrode is added to the system. In this setup, the working

electrode is what is being measured, the counter electrode acts as a current source, and the reference electrode holds a constant potential. This allows for more applications and a more confident reading, and accuracy compared to the two-electrode system [35]. For a four-electrode system, a working sense electrode is implemented into the system. With this configuration, the reactions at the working electrode are not being measured. Instead the effect of the current of the solution itself is being measured [35].

2.4 References

[1]. S. Li, Y. Wang, J. Zhou and F. Xue, "Investigation of jet printing performance of lead-free solder paste," International Conference on Electronic Packaging Technology (ICEPT), pp. 709-712, 2016.

[2]. A. Kamyshny, S. Magdassi, “Conductive Nanomaterials for Printed Electronics”, Small, vol. 10(17), pp.3515-3535, 2014.

[3]. J. Chang, T. Ge and E. Sanchez-Sinencio, "Challenges of printed electronics on flexible substrates," Midwest Symposium on Circuits and Systems (MWSCAS), Boise, pp. 582-585, 2012.

[4]. B. B. Narakathu, “Integration of conventional lithography and printing processes as a key enabling technology for printed and flexible sensing system”. PhD. Dissertation, Western Michigan University, Ann Arbor: ProQuest, 2014

[5]. V. S. Turkani, “Implementation of Additive Print Manufacturing Processes for the Development of Flexible Thermal Sensors”, Master’s Theses, Western Michigan University, 2018

[6]. F. Harrer, F. Pfeiffer, A. Löffler, “Automotive Synthetic Aperture Radar System Based on 24 GHz Series Sensors”, Advanced Microsystems for Automotive Applications, 2017.

[7]. Q. Xu, L. Cheng, L. Meng, “Flexible Self-Powered ZnO Film UV Sensor with a High Response”, ACS Applied Materials & Interfaces, vol. 11(29), pp. 26127-26133, 2019.

[8]. D. Maddipatla, B. B. Narakathu, S. G. R. Avuthu, S. Emamian, A. Eshkeiti, A. A.Chlaihawi, B. J. Bazuin, M. K. Joyce, C. W. Barrett, M. Z. Atashbar, “A novel flexographic printed strain gauge on paper platform”, 14th IEEE Sensors Conference, November 1-4, Busan, South Korea, 2015.

[9]. A. S. G. Reddy et al., “Fully printed organic thin film transistors (OTFT) based flexible humidity sensors,” Proc. IEEE Sens., pp. 1-4, 2013.

[10]. V. S . Turkani,D. Maddipatla, B.B. Narakathu, B.J. Bazuin, and M.Z. Atashbar, “A Carbon Nanotube Based NTC Thermistor using Additive Print Manufacturing Processes” Sensors and Actuators A: Physical. 279, 15, 1-9, 2018, https://doi.org/10.1016/j.sna.2018.05.042

[11]. A. S. G Reddy et al., “Printed electrochemical based biosensors on flexible substrates,” Proc. IEEE Sens., pp. 1596-1600, 2010.

[12]. D. Maddipatla et al., "Development of a Flexible Force Sensor using Additive Print Manufacturing Process," 2019 IEEE International Conference on Flexible and Printable Sensors and Systems (FLEPS), pp. 1-3, 2019.

[13]. S. Harada, K.Kanao, Y.Yamamoto, “Fully Printed Flexible Fingerprint-like Three-Axis Tactile and Slip Force and Temperature Sensors for Artificial Skin”, ACS Nano, pp. 12852-12857, 2014.

[14]. D. Birchfield, X. Jackson, T. Pasternak, A. Hanson and M. Atashbar, "Strain Sensor Fabrication by Means of Laser Carbonization", 2019 IEEE International Conference on Flexible and Printable Sensors and Systems (FLEPS), pp. 1-3, 2019.

[15]. M. Atashbar, M. Joyce, B. Narakathu, “Helmet Impact Monitoring System”, US Patent 9,943,128, 2018.

[16]. T. Holleczek, A. Rüegg, H. Harms and G. Tröster, "Textile pressure sensors for sports applications," SENSORS, 2010 IEEE, pp. 732-737, 2010.

[17]. J. Pörhönen, S. Rajala, S. Lehtimäki and S. Tuukkanen, "Flexible Piezoelectric Energy Harvesting Circuit with Printable Supercapacitor and Diodes," in IEEE Transactions on Electron Devices, vol. 61(9), pp. 3303-3308, 2014.

[18]. S. Emamian et. Al. “Fully printed and flexible piezoelectric based touch sensitive skin”, 14th IEEE Sensors Conference, November 1-4, Busan, South Korea, pp. 1827-1830, 2015.

[19]. J. Chang, G. Zhou, E. Christensen, “Graphene-based sensors for detection of heavy metals in water: a review”, Analytical and Bioanalytical Chemistry, vol. 406(16), pp. 3957-3975, 2014.

[20]. E. Krommenhoek, J. Gardeniers, J. Bomer, “Monitoring of yeast cell concentration using a micromachined impedance sensor”, Sensors and Actuators B: Chemical, vol. 115(1), pp. 384-389, 2006.

[21]. A. Romeo, A. Moya, T. Leung “Inkjet printed flexible non-enzymatic glucose sensor for tear fluid analysis”, Applied materials today, vol. 10, pp. 133-141, 2018.

[22]. S. G. R. Avuthu *et al*., "Detection of heavy metals using fully printed three electrode electrochemical sensor," *IEEE Sensors*, pp. 669-672, 2014.

[23]. D. Maddipatla, B. B. Narakathu, B. J. Bazuin and M. Z. Atashbar, "Development of a printed impedance based electrochemical sensor on paper substrate," IEEE SENSORS, pp. 1-3, 2016.

[24]. A.S.G. Reddy, B.B. Narakathu, M.Z. Atashbar, “Gravure Printed Electrochemical Biosensor”, Procedia Engineering, vol. 25, pp. 956-959, 2011.

[25]. B. B. Narakathu, M. Z. Atashbar, B. E. Bejcek " Pico-mole level detection of toxic bio/chemical species using impedance based electrochemical biosensors ," Sensor Letters 9 (2), 872-875.

[26]. A. S. G. Reddy, B. B. Narakathu, M. Z. Atashbar, M. Rebros, E. Hrehorova and M. Joyce, "Printed electrochemical based biosensors on flexible substrates,"*IEEE Sensors*, pp. 1596-1600, 2010.

[27]. B.B. Narakathu, M.Z. Atashbar, B.E. Bejcek, “Improved detection limits of toxic biochemical species based on impedance measurements in electrochemical biosensors” Biosensors and Bioelectronics, vol. 26(2), pp. 923-928, 2010.

[28]. B.B. Narakathu *et al*., " Novel fully screen printed flexible electrochemical sensor for the investigation of electron transfer between thiol functionalized viologen and gold clusters”, Sensors and Actuators B: Chemical, vol. 176, pp. 768-774, 2013.

[29]. A. Abellan-Llobregat, I. Jeerapan, A. Bandodkar, “A stretchable and screen-printed electrochemical sensor for glucose determination in human perspiration”, Biosensors and Bioelectronics, vol. 91, pp. 885-891, 2017.

[30]. A. Pal, H. Cuellar, R. Kuang, “Self-Powered, Paper-Based Electrochemical Devices for Sensitive Point-of-Care Testing”, Advanced Materials Technologies, vol. 2(10), 2017.

[31]. A. K. Bose, D. Maddipatla, B. B. Narakathu, B. J. Bazuin and M. Z. Atashbar, "Laser-Assisted Patterning of a Flexible Microplasma Discharge Device for Heavy Metal and Salt Detection in Ambient Air," 2019 IEEE International Conference on Flexible and Printable Sensors and Systems (FLEPS), pp. 1-3, 2019.

[32]. M. Pumera, A. Ambrosi, A. Bonanni, “Graphene for electrochemical sensing and biosensing”, TrAC Trends in Analytical Chemistry, vol. 29(9), pp. 954-965, 2010.

[33]. A. Issac, J. Davis, C. Livingstone, “Electroanalytical methods for the determination of sulfite in food and beverages” TrAC Trends in Analytical Chemistry, vol. 25(6), pp. 589-598, 2006.

[34]. D. Han, W. Ma, L. Wang, S. Ni, “Design of two electrode system for detection of antioxidant capacity with photoelectrochemical platform”, Biosensors and Bioelectronics, vol. 75, pp. 458-464, 2016.

[35]. Gamry Instruments, “Two, Three and Four Electrode Experiments”, [Online]. Available: https://www.gamry.com/application-notes/instrumentation/two-three-and-four-electrode-experiments. [Accessed: 26- Oct- 2019].

CHAPTER 3

PORTABLE ELECTROCHEMICAL SYSTEM

3.1 Introduction

It has been proven that electrochemical sensing methods can detect and quantify the concentration of glucose using a large stationary machine in a laboratory environment [1-5]. To design an all-in-one system, an electronic readout had to be designed that would keep the major functions of the system while being able to fit in the palm of a hand. The idea is that this device could be turned into a biosensing patch on a human body if proven that it can be portable while still being reliable. Many tasks were involved in making this system ranging from the sensor to the electronics to the variety of tests being performed. These tasks will be described in detail in this chapter.

3.2 Experimental

This section will discuss how the author designed and fabricated a three-electrode sensor and developed a portable electronic read out unit for the sensor.

3.2.1 Sensor Design

For developing a three-electrode sensor, the design was based on a printed electrochemical sensor reported previously [6]. The design was made in Autodesk AutoCAD 2019 and was 2 cm by 1 cm (Fig. 3.1). The contact pads were placed 3.85 mm apart to match the profile of the connector for the electronic read out. All sharp (90 degree) corners were rounded to allow for easier fabrication, which is different from the

reference design. The sensor consisted of counter, working, and reference electrodes (Fig. 3.1).

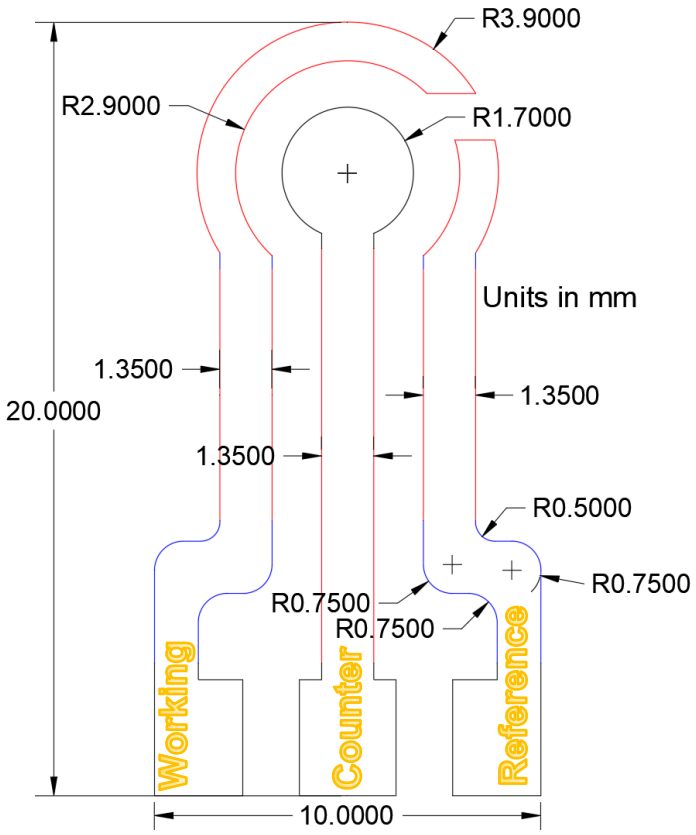

Figure 3.1. Schematic of three-electrode sensor.

3.2.2 Sensor Fabrication

To fabricate the sensor, the process of laser etching was used. A 6 MW fiber laser from Universal Laser Systems was used to pattern the design out of copper tape (Bertech CFT-2). This sensor was a two-layer design (Fig. 3.2). The bottom layer was the polyethylene terephthalate (PET) substrate while the top layer was the copper tape. After several attempts of changing the laser parameters to pattern the sensor, a burning problem occurred in some areas. To fix this, the design was broken up into 3 sections

each containing a different color (black, blue, and red) (Fig 3.1). Each color had different laser parameters (power and speed) therefore the areas that were burning could be reduced in power. After this fix, the sensor was fabricated as designed. Once the sensor was patterned with the laser machine, tweezers were used to pull away the unwanted copper (Fig 3.3).

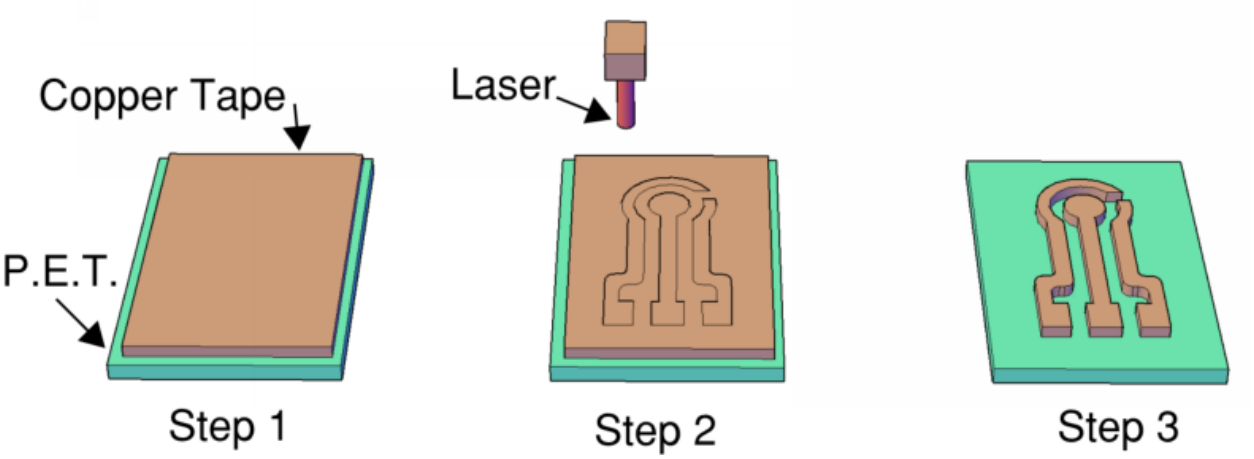

Figure 3.2 Fabrication steps for three-electrode sensor.

Figure 3.3 Photograph of fabricated sensor.

3.2.3 Electronics

To preform electrochemical sensing with a low power consumption, Texas Instruments programmable Analog Front End (AFE) potentiostat LMP91000 IC was used. This IC is an analog front-end circuitry that is specifically designed for electrochemical voltammetry applications. The device operates on 2.7 V – 5.25 V

supply voltage and uses a low amount of current less than 10 µA while having key features like programmable cell bias and programmable transimpedance amplifier gain [7]. This IC then is interfaced with a microcontroller as shown in figure 3.4 which sets the parameters via I2C communications and reads the output voltage. The microcontroller used was the Adafruit Feather nRF52832. This controller was used because of its small size (22.86 mm by 50.8 mm), low power consumption (5.3uW), 12-bit analog to digital converter (ADC), and Bluetooth low energy (BLE) compatibility

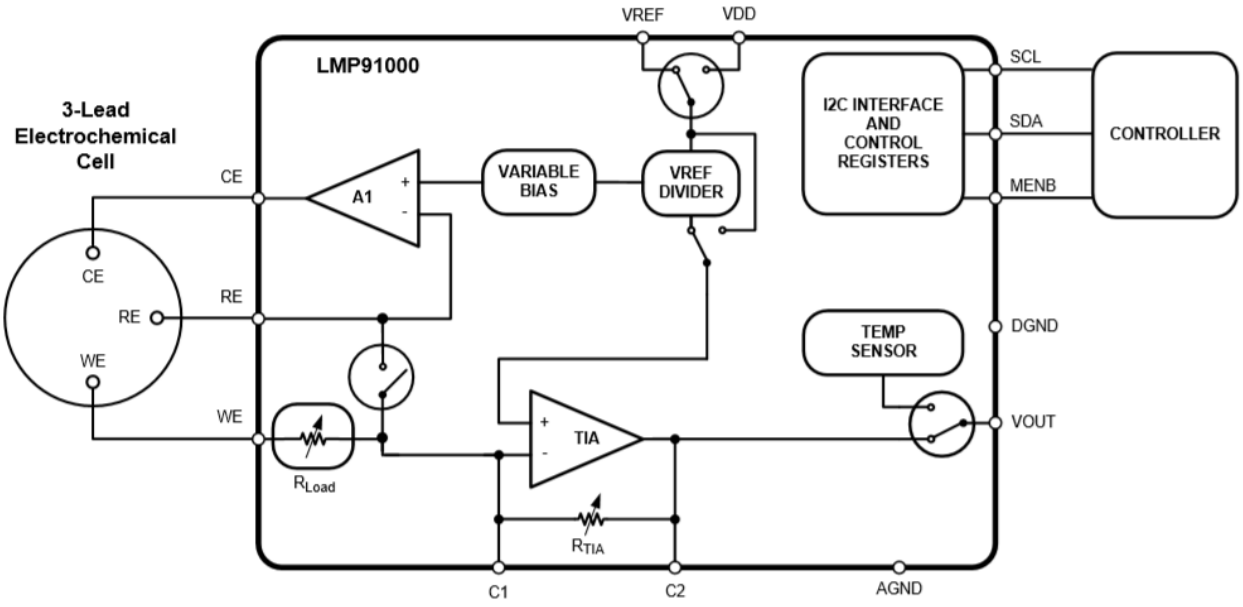

Figure 3.4 Schematic of the LMP91000 IC [7].

After a working prototype was built, a custom printed circuit board (PCB) was designed using Autodesk Eagle 2019. This board included the LMP91000 IC for electrochemical sensing and the nRF52832 to configure the LPM91000 and wirelessly transmit the results. The microcontroller contained a reset button as well as a DTR option for programing. There is also a 32.768 oscillation crystal attached to the microcontroller (Fig 3.5).

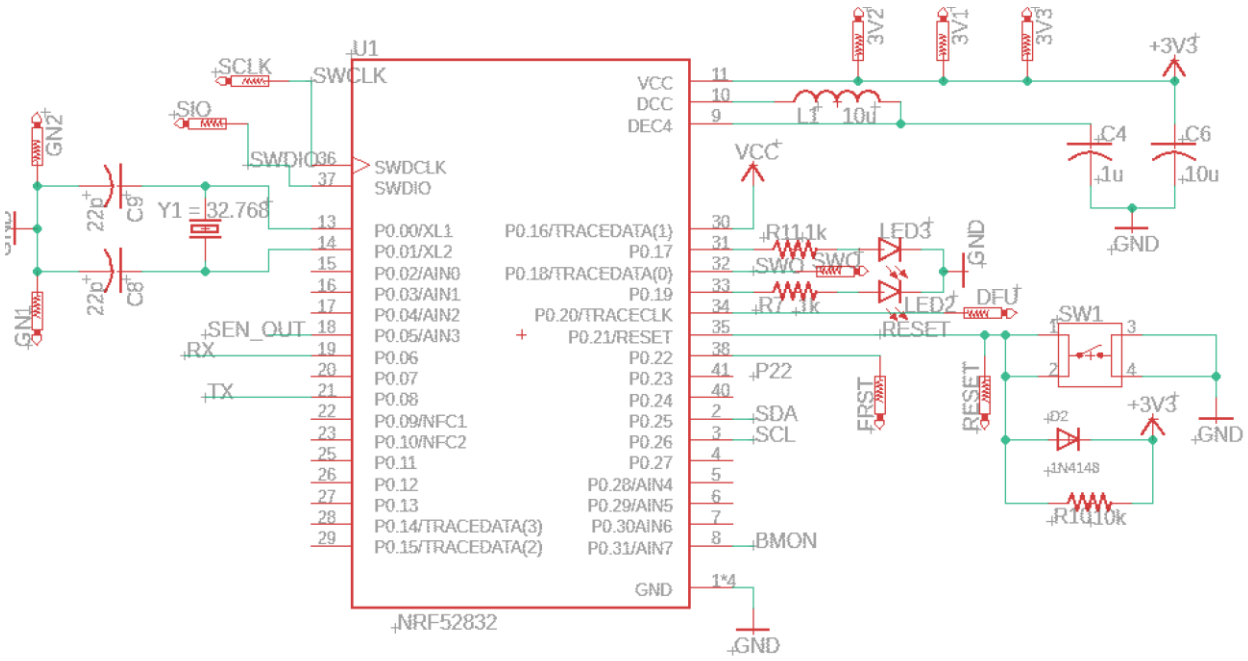

Figure 3.5 Schematic of the microcontroller unit.

The LMP91000 was connected to the microcontroller via I2C with two pull up resistors to remove the chance of error during communication (Fig 3.6).

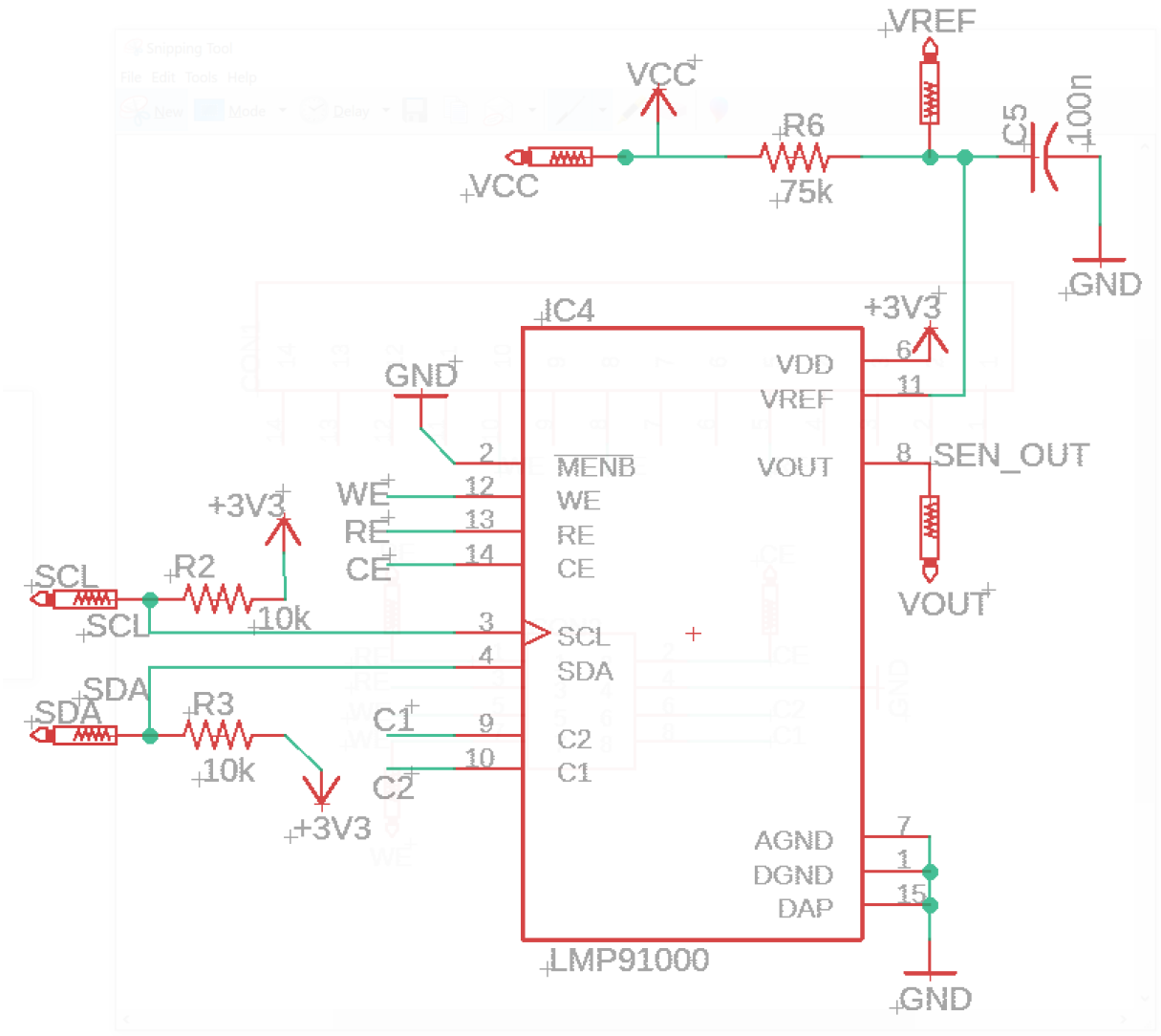

Figure 3.6 Schematic for the electrochemical sensing circuit.

The reference voltage applied to the LMP91000 can either be internal (3.3 V) or external. For external, an RC circuit was added which was being controlled by the microcontroller using PWM which operated at a frequency of 64 kHz (Fig 3.7). A simulation was performed to find the time it takes to reach its saturation level (Fig 3.8). With this information, a delay of 20 ms was implemented into the program before the program starts to set the reference voltage. The simulation also showed the variation in the reference voltage to be about 1.7 mV (Fig 3.9).

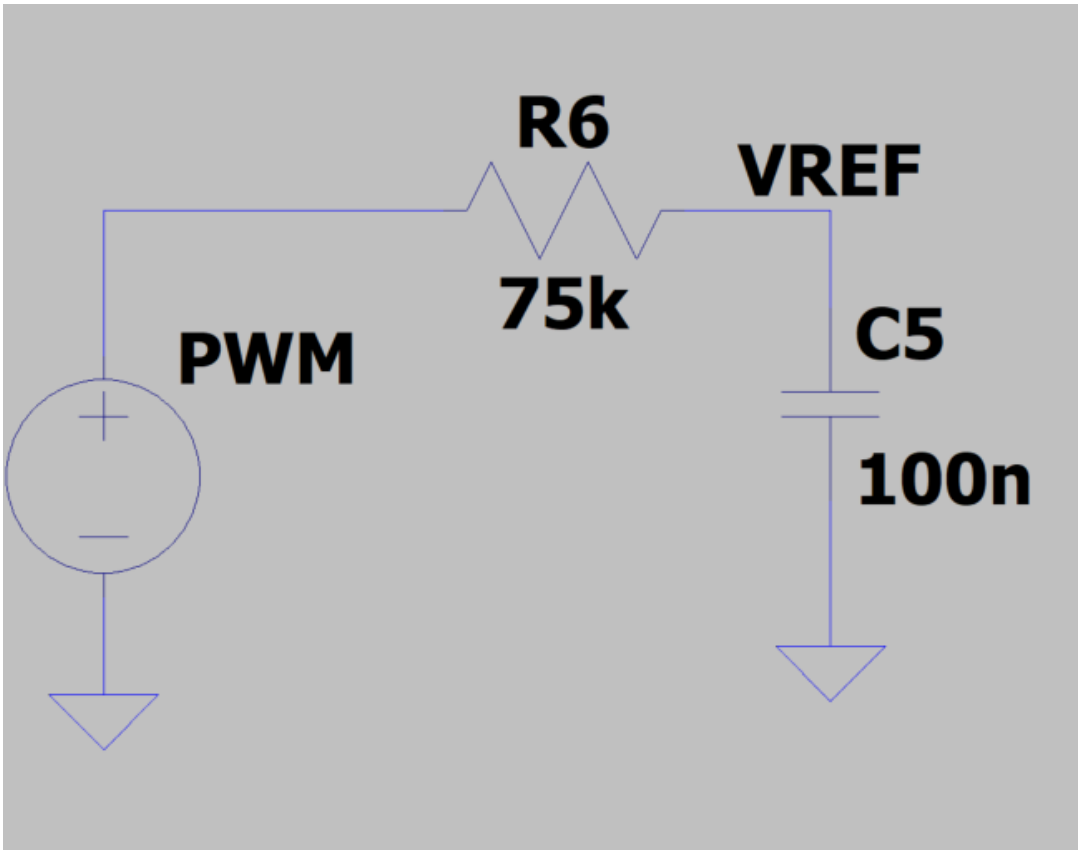

Figure 3.7 Schematic of the reference voltage circuit.

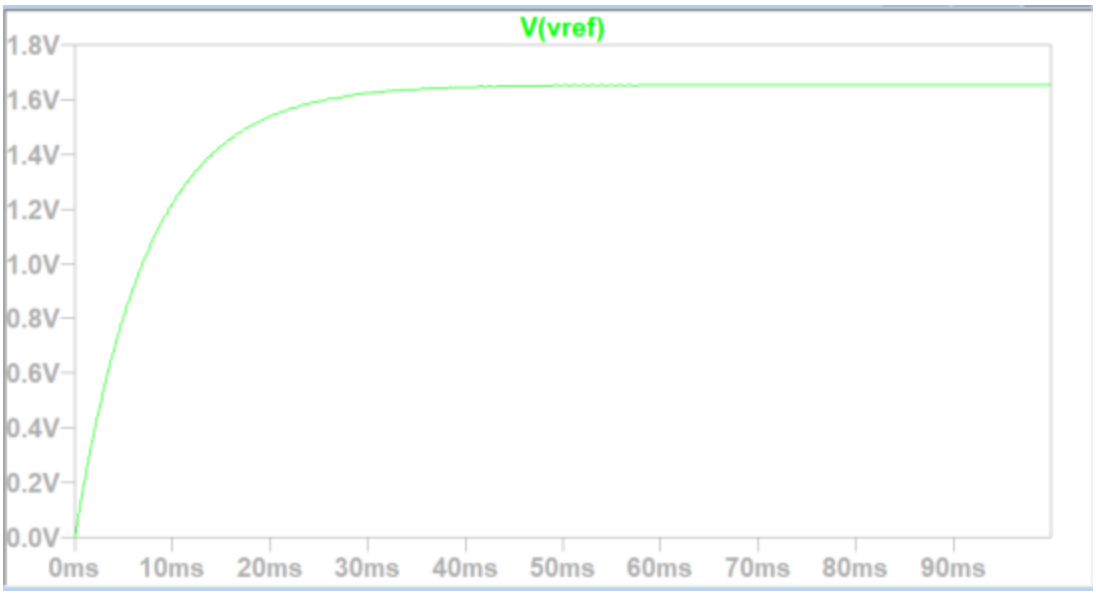

Figure 3.8 Simulation of the reference voltage reaching saturation.

Figure 3.9 Simulation of the reference voltage variation.

Another feature on the board was a battery charging and monitoring circuit, so the that battery never has to be removed from the system (Fig 3.10).

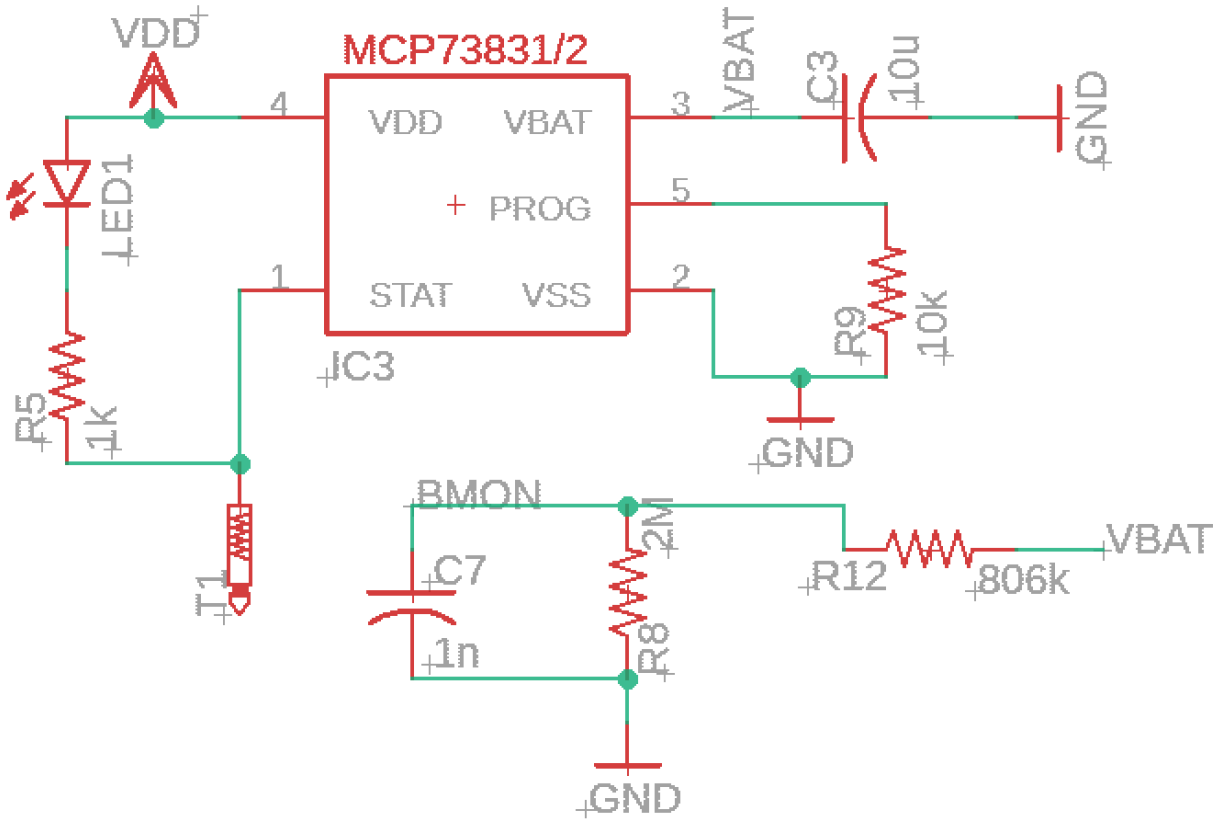

Figure 3.10 Schematic of battery charging and battery monitoring circuit.

To filter the power, a 3.3 voltage regulator was added, and a DMG3415 MOSFET was used to switch between battery and USB power (Fig 3.11).

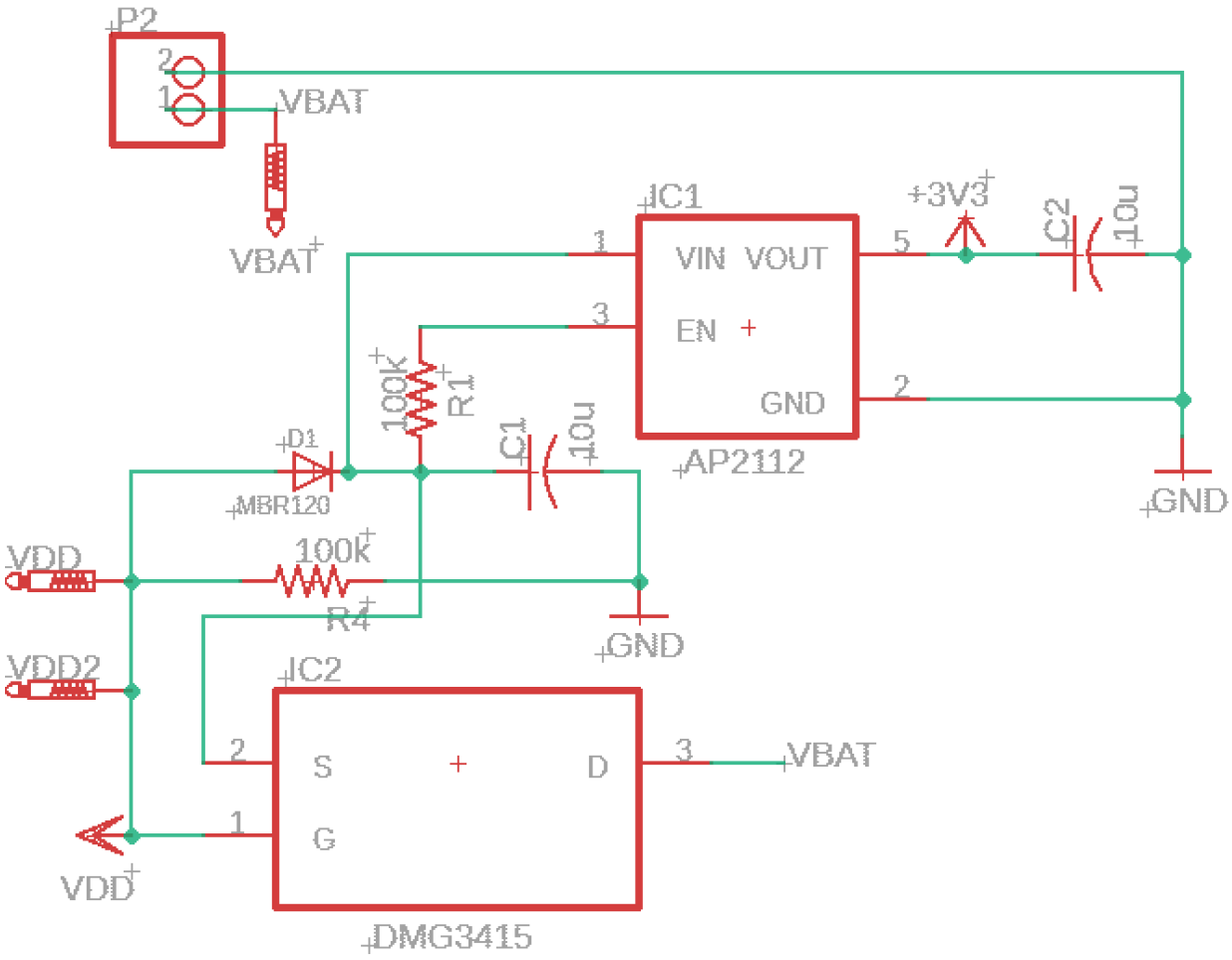

Figure 3.11 Schematic of the power filtering.

The board also contained two different connectors for the sensor. The main connector was a zero-insertion force (ZIF) connector that was for the three-electrode sensor. The other connector was a pin header so any external sensor could be tested with it. By shorting the reference and counter pins in the header, a two-electrode sensor could be used (Fig 3.12).

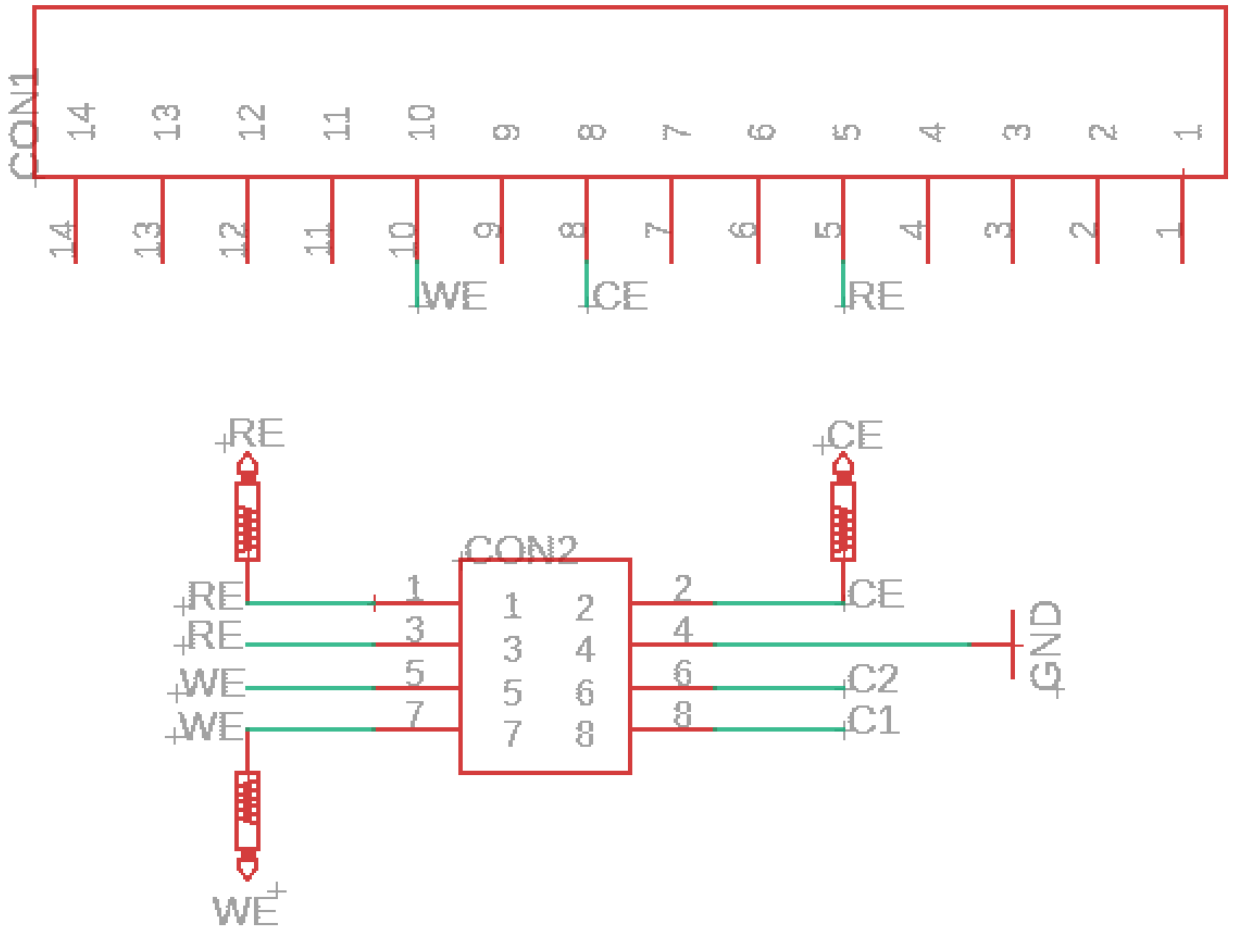

Figure 3.12 Schematic for the external connectors.

The board could be programed through JTAG pins or the more convenient way, through a micro USB cable. This could be done through the onboard USB to UART bridge (Fig 3.13).

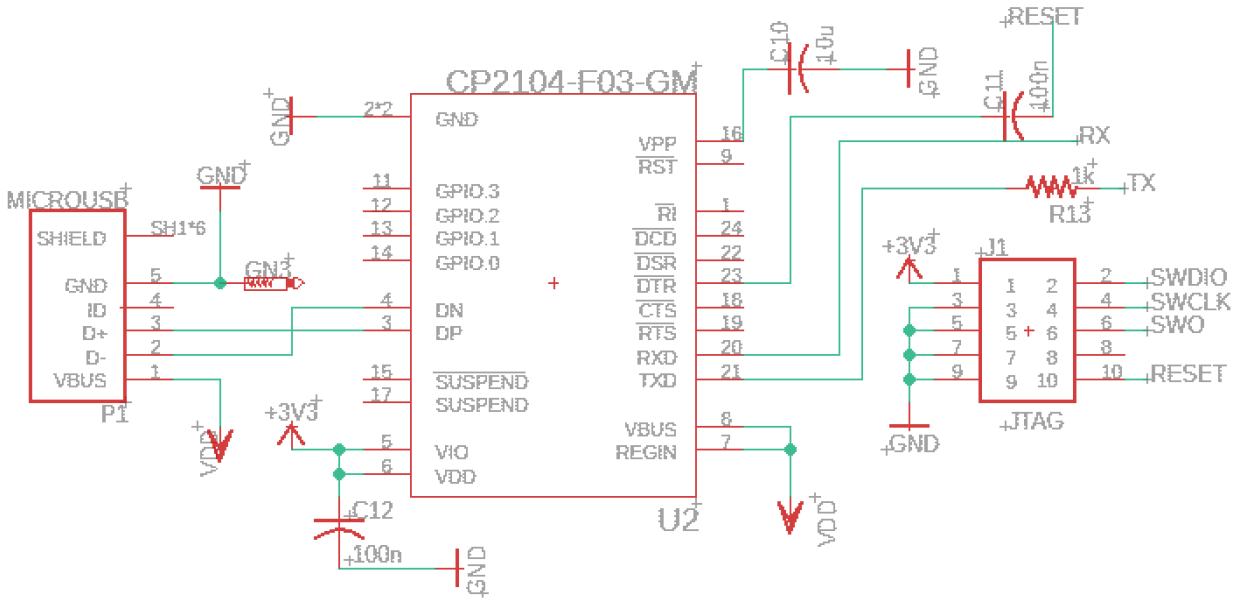

Figure 3.13 Schematic of the device programing circuit.

There are also 3 LEDs on the board which can be used in the program or turned off to save power consumption. Currently, 1 LED is used to show if the battery is charging or not, another LED is used to show BLE connectivity, and the final LED shows if a test is in progress of not. The schematic of the entire system can be seen in figure 3.14.

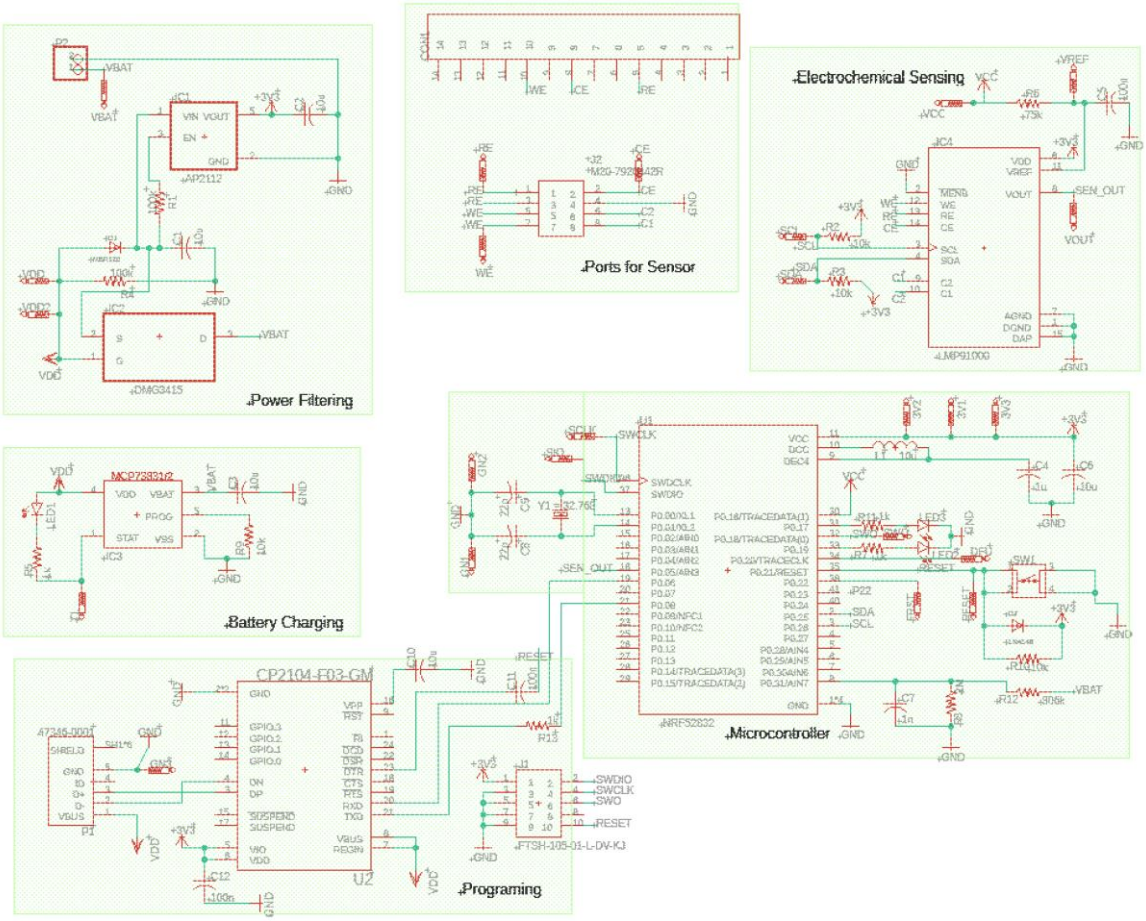

Figure 3.14 Schematic of Portable Electrochemical System.

The PCB included 3 mm holes which were placed in three corners of the board to allow for locking-in-place if a protective cover was used. To reduce the noise in the circuit, a ground plane was added throughout the board. For simplicity in production and cost reduction, the board was designed for only two layers. With being only two layers, the applications for this device are more open because the board can be manufactured on a flexible polyimide material like Kapton instead of the traditional fiberglass. With all these hardware features, the overall PCB dimension is 51 mm by 62 mm which is smaller than an average adult hand (Fig 3.15).

Figure 3.15 Photograph of the Portable Electrochemical System.

3.2.4 Calibration

After the sensor circuit were fabricated, the system was calibrated. The calibration was completed in two parts: making the code for the system and using a graphing program for post analysis the recorded data. The code for the program was written in C++ using the Arduino IDE and the flowchart of the program is shown in figure 3.16. Source code is provided in appendix.

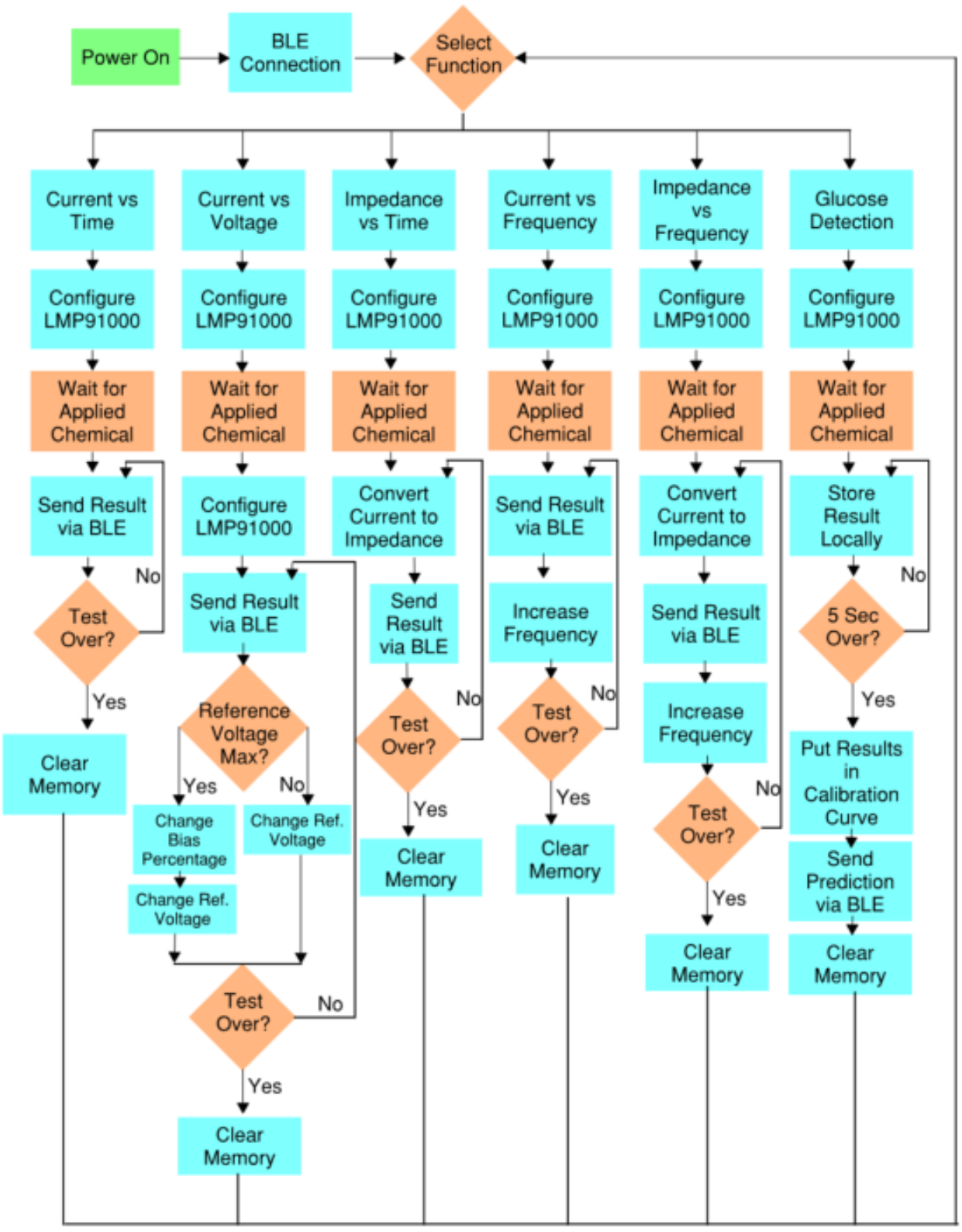

Figure 3.16 Flowchart for the program used on the microcontroller.

The LMP91000 was configured using a multi-step process which included: TIA gain, load resistance, reference source, internal zero, bias sign, bias voltage, mode, frequency, number of points, and accuracy. Since this was a multi-step process, the author developed custom algorithms for automating this process. The user can choose between six different tests. These include current vs time, current vs voltage, impedance vs time, current vs frequency, impedance vs frequency, and a glucose detection mode. With these configurations the user now only must select the test, TIA gain, frequency, and length of test. For the TIA gain, there are seven preset gains, and the PCB also features the ability to make a custom gain through the pin head connector. The higher the gain the lower the concentration that can be detected and the lower the gain the higher the concentration can be detected. Since there is no way to tell which gain is needed until the test is running, an automatic gain setter was implemented in the code to find the optimal gain for testing chemicals in just moments after the chemical was applied to the sensor. This feature also adds the ability to increase or decrease the gain automatically during the test. This is very useful for tests like cyclic voltammogram. With these software features, the user now must select only the test type, desired frequency (if required), and the length of the test. To make sure these graphs and reading are correct, the results were compared with previous work [8].

If the user does not want to run the test, and instead want to know only the concentration of glucose, this can be done as well. For initial calibration, tests with the current vs time mode for a length of five seconds was done (Fig 3.17). A five second time interval is used because the initial current recorded is affected by the velocity of the

chemical being applied to the sensor. After five seconds, the sensor response stabilizes enough to have an accurate and consistent reading. Testing multiple different known concentrations of glucose helped get a clear calibration curve which. Now the user could do a drop test of glucose mixed with deionized (DI) water and find the glucose concentration.

Figure 3.17 Pipette to drop the glucose sample onto the sensor.

3.3 Results and Discussion

During a test where the results would be wirelessly transmitted to a smartphone, the systems uses about 2.8 mA. When there is no test running, the system uses about 1.6 mA. This means that with a small 400 mAH lithium polymer battery, while running a test every minute, the system would last roughly 9.8 days. This device would therefore

work for applications that require a working duration of one week. This time could be increased by reducing the test rate or by increasing the battery size.

The program functions were tested, and the results are shown below. Figure 3.18 shows the test results for the cyclic voltammogram mode for a 1 mM glucose in DI water. Different scan rates were used due to a combination between the present LMP91000 biases and the variable reference voltage that was implemented on the custom PCB. A frequency sweep test was performed to find the best sample frequency for glucose. The largest delta between the concentrations will give the best accuracy when predicting the concentration. It was observed there was not much of a change throughout the frequency of 1 Hz to 1 kHz (Fig. 3.19). This is because the maximum sample rate for the device is 1 kHz and therefore a change in delta might have appeared at higher frequencies. The device was then set to a sampling frequency rate of 100 Hz. Figure 3.20 shows the chronoamperogram (current vs time) of different concentrations of glucose. Figure 3.21 shows the calibration curve that was created for the data. Each concentration was tested 6 times and the average was used in the calculations for the calibration curve.

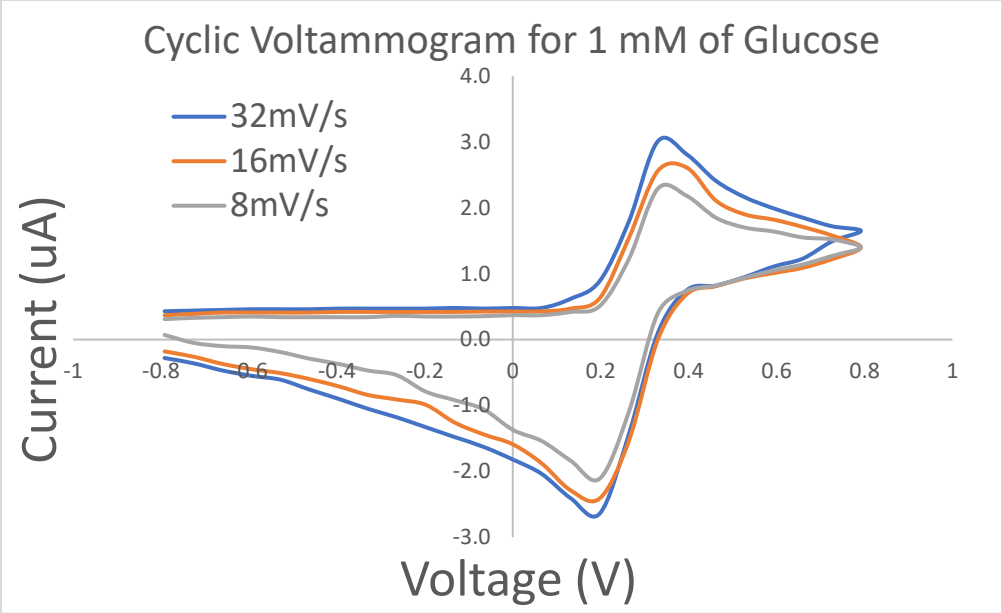

Figure 3.18 Cyclic voltammogram for 1 mM of glucose.

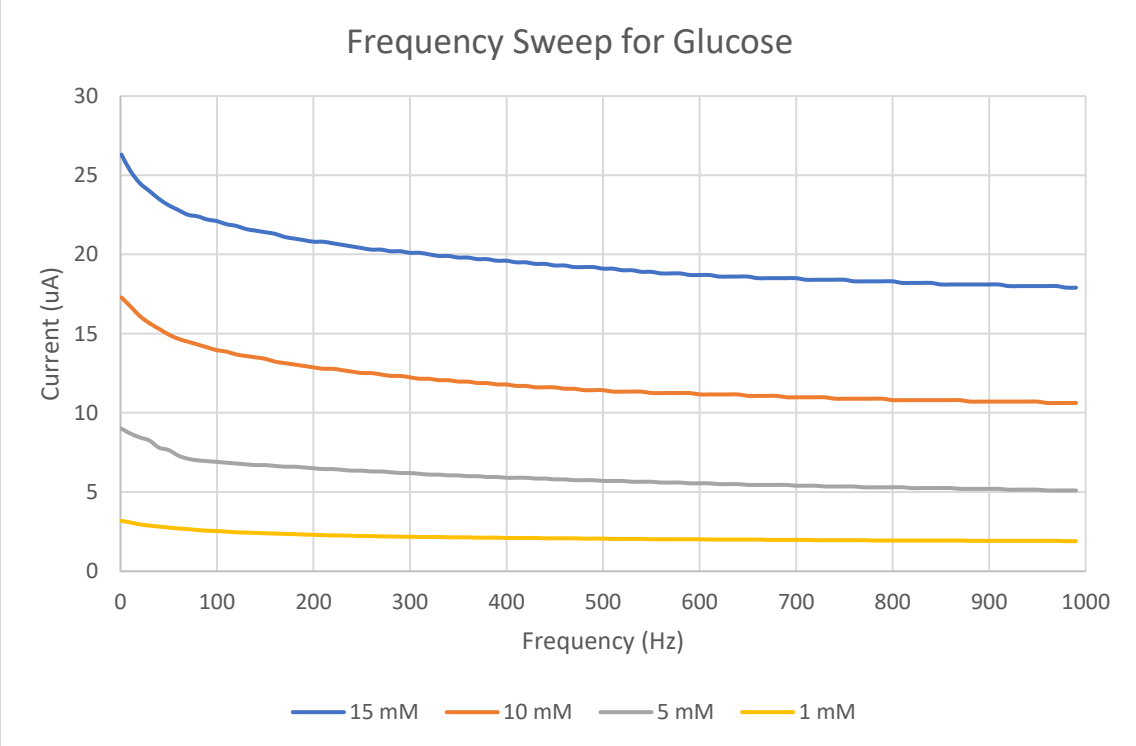

Figure 3.19 Frequency sweep from 1 Hz to 1 kHz.

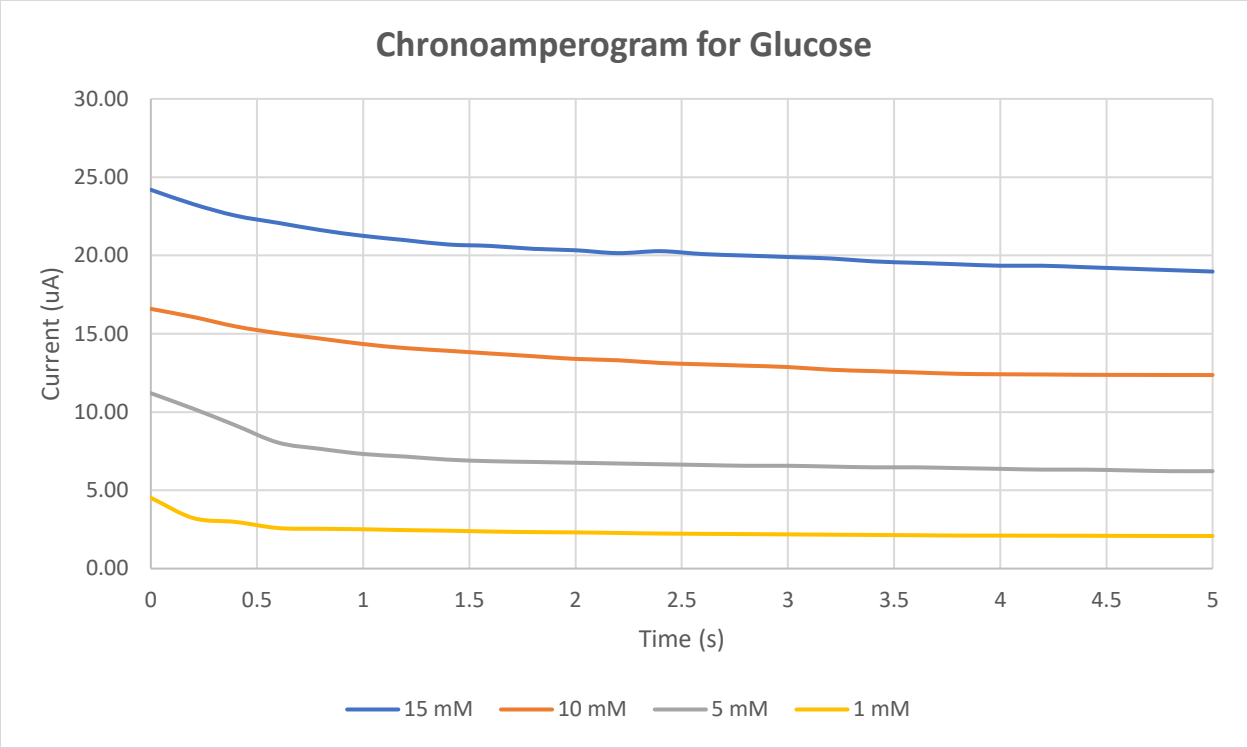

Figure 3.20 Chronoamperogram for various concentrations of glucose.

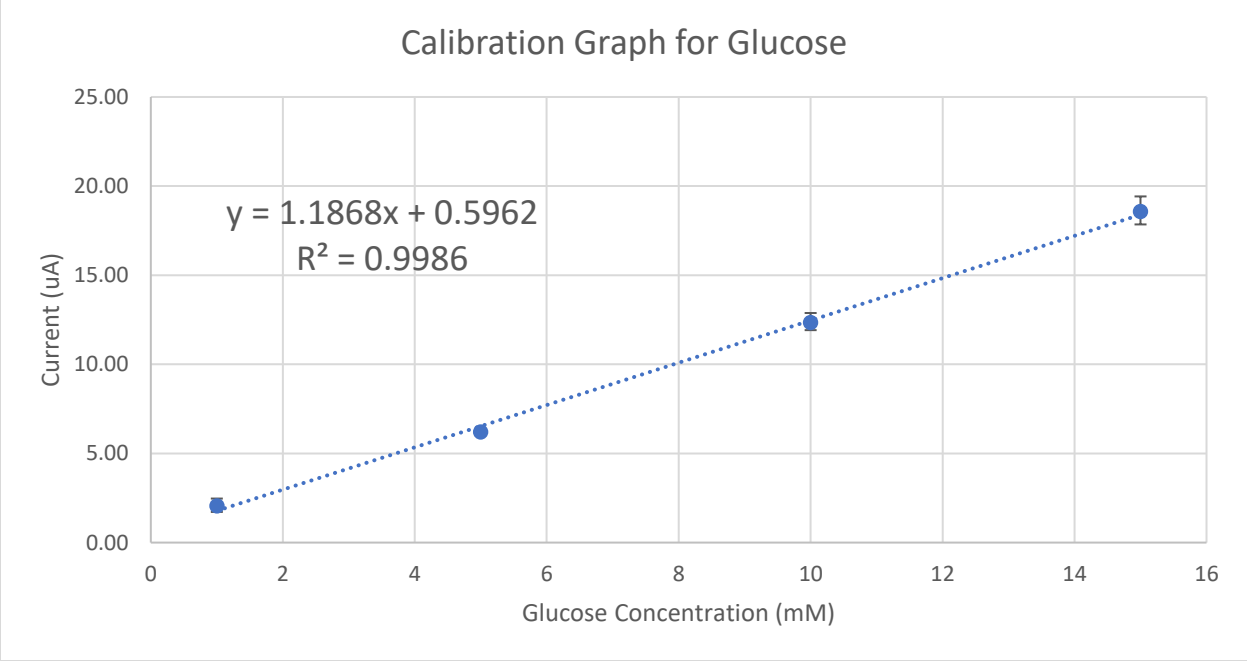

Figure 3.21 Calibration curve used to detect glucose concentrations.

A mixture of 7 mM of glucose was made to test the calibration curve. For this test, four trials were performed. Table 3.1 shows the results for each of the test. Averaging those numbers gives a reading of 7.21 mM which has a 2.96% error. A possible reason for the error and different predictions between test can be the velocity that the fluid is put onto the sensor or the location it was applied to. Through observation, when the velocity of the applied chemical was large, a slightly larger chemical reading would appear compared to a slow velocity. The large velocity could be shifting the copper tape, or the chemical could be going under the tape as well. When applying the chemical with a slow velocity, the chemical reaction starts before all the sensor is covered. This could be better controlled using an automated process which would apply the fluid with the same velocity to the sensor and in the same location each time. Another reason for the 2.96% error can be due to the open sensor design. This design makes the processes simpler to apply the chemical solution however, it also can add noise to the system. Since the system is reading very small current (microamperes), the results could vary slightly between tests.

Table 3.1. Prediction results for 7 mM of glucose based on calibration curve.

	Trial 1	**Trail 2**	**Trail 3**	**Trail 4**
Prediction (mM)	7.08	6.94	7.56	7.25

The system was also tested using a two-electrode sensor attached to the pin header. For this test, sodium chloride (NaCl) was used in concentrations of 1 pM, 1 nM, 1 uM, and 1 mM. The device was able to read the current passing through the two electrodes (Fig. 3.22).

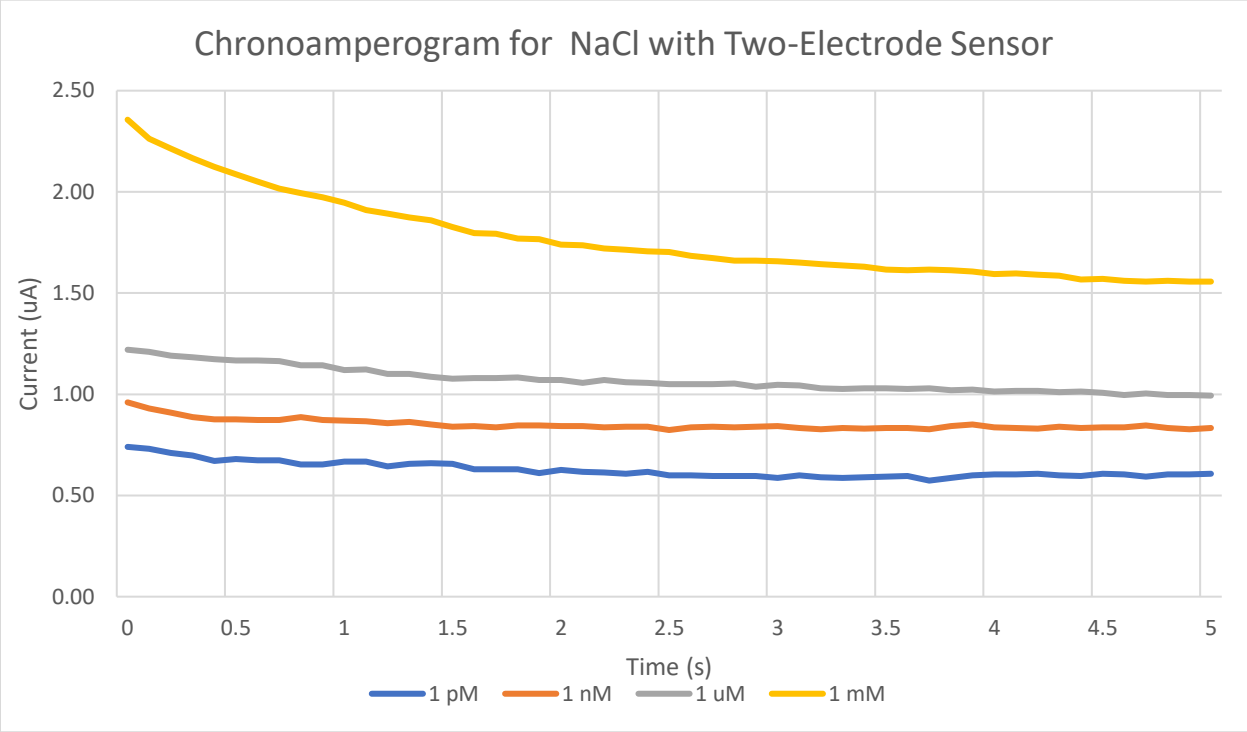

Figure 3.22 Chronoamperogram using a two-electrode sensor testing NaCl.

3.4 References

[1]. D. Maddipatla, B. B. Narakathu, B. J. Bazuin and M. Z. Atashbar, "Development of a printed impedance based electrochemical sensor on paper substrate," *IEEE SENSORS*, pp. 1-3, 2016.

[2]. A.S.G. Reddy, B.B. Narakathu, M.Z. Atashbar, “Gravure Printed Electrochemical Biosensor”, Procedia Engineering, vol. 25, pp. 956-959, 2011.

[3]. B. B. Narakathu, B. E. Bejcek and M. Z. Atashbar, "Impedance based electrochemical biosensors," *IEEE Sensors*, pp. 1212-1216, 2009.

[4]. A. S. G. Reddy, B. B. Narakathu, M. Z. Atashbar, M. Rebros, E. Hrehorova and M. Joyce, "Printed electrochemical based biosensors on flexible substrates", IEEE Sensors, pp. 1596-1600, 2010.

[5]. B.B. Narakathu, M.Z. Atashbar, B.E. Bejcek, “Improved detection limits of toxic biochemical species based on impedance measurements in electrochemical biosensors” Biosensors and Bioelectronics, vol. 26(2), pp. 923-928, 2010.

[6]. S. G. R. Avuthu *et al*., "A Screen Printed Phenanthroline-Based Flexible Electrochemical Sensor for Selective Detection of Toxic Heavy Metal Ions," *IEEE Sensors*, vol. 16(24), pp. 8678-8684, 2016.

[7]. Texas Instruments, “LMP91000 Sensor AFE System: Configurable AFE Potentiostat for Low-Power Chemical-Sensing Applications”, LMP91000 datasheet, Jan. 2011 [Revised Dec. 2014].

[8]. A. Pal, H. Cuellar, R. Kuang, “Self-Powered, Paper-Based Electrochemical Devices for Sensitive Point-of-Care Testing”, Advanced Materials Technologies, vol. 2(10), 2017.

CHAPTER 4

FUTURE WORK AND CONCLUSION

4.1 Future Work

The author has a few ideas that could help further improve the project.

- By creating a flow cell, this can control the analyte volume on the sensing area of the sensor. This should improve the error for predicting the concentration of a glucose.
- The printed circuit board was made with traditional fiberglass. To further Advance the use of this system in a variety of applications, the printed circuit board can be Kapton based to provide flexibility. This would open the door for bio-applications including patches on a human body or sensing chemicals on a curved surface like a water bottle or food container.
- A custom smartphone application can be developed that would make the user interface much simpler. Currently, a BLE terminal is being used and the user must know the commands to adjust the parameters and start the program.
- To make a full biosensing system, more chemicals than just glucose needs to be detected. Adding multiple sensors to the system and running simultaneous tests with each sensor calibrated for a different chemical would be a viable improvement.

4.2 Conclusion

Overall, the author developed a portable electronic device that was able to detect different concentrations of glucose using a sensor that was made with FHE fabrication

techniques. With this device, electrochemical sensing can be done anywhere, not just a laboratory, in a matter of 5 seconds and be recorded wirelessly using a smart phone. The portable electrochemical device is low-cost which can largely improve the available applications for chemical detection with FHE sensors.

In summary, a three-electrode sensor was fabricated using copper tape on a PET substrate. The design was precisely patterned using a fiber laser machine. The electrical circuit consisted of two main parts: the Nordic Semiconductor nRF52832 microcontroller and Texas Instruments LMP91000 IC. The LMP91000 IC was the front end for electrochemical sensing and the nRF52832 microcontroller was performing the calculations and transmitting the wireless signal. The electronics also include two power options (3.7V battery or a micro USB cable), a battery monitoring and charging circuit, and the ability to use an external sensor. The device could be configured for two and three-electrode sensors, has the ability to change the potential across the sensor, and could also change the sampling rate for the system. The program could be used for testing purposes by creating a current vs time graph or be used to detect the concentration of a chemical after properly obtaining a calibration curve. This system proved that it was able to detect glucose concentrations.

With the knowledge gained from this thesis, the author learned a great deal about FHE and the potential they have for future applications. There is a large area for research in this field, for both the sensors and electronic read out systems. Having the knowledge of how the sensors perform, knowing the acquisition methods required, and the different fabrication methods is a great start to being able to make the electronic readout systems required to make consumer products, but there is much more still to

learn. The author would like to learn more about the emerging field of FHE by working for a company that has a background in FHE or is interested in starting a product using FHE.

APPENDIX

Code For Microcontroller

```
#include <Wire.h>
#include <bluefruit.h>
#include "LMP91000.h"
#define sensor A3
#define MENB 7
#define vref 16


/*Enter the Parameters Here*/
//TIA..2P75K,3P5K,7K,14K,35K,120K,or 350K.. RLoad 10,33,50,100
//Reference Control source = INT,EXT..Z = 20PCT,50PCT,67PCT..Sign = POS,NEG..Bias = 0PCT,1PCT,2PCT,4PCT,6PCT,8PCT -> 24PCT
uint8_t TiaSet = TIA_350K;
uint8_t RSet = RLOAD_33;
float vrefVoltage = 0.0; // must be between 1.5 and vdd. Use 0.0 if using Ref_Source_INT.
uint8_t IntSet = INT_Z_50PCT;
uint8_t SignSet = BIAS_SIGN_POS;
uint8_t BiasSet = BIAS_14PCT;
uint8_t FetSet = FET_SHORT_DISABLED;
uint8_t ModeSet = MODE_AMPEROMETRIC;
int function = 0; // 0=current vs time, 1=current vs voltage, 2 = impedence vs time, 3 = current vs frequency, 4 = impedence vs freq,
//5 curr and imp vs time, 6 curr and imp vs freq, 7 is chemical detection for KCL
int accuracyVolt = 20; //how many mV/s
//int delayVoltamm = 330; //Delay inbetween samples for voltamm, only matters if Function is 1
int delayTime = 100;// Sample frequency if Function is set to 0
float vdd = 3.30; //Constant voltage going to vdd on the lmp91000.
```

```
bool autoCali = 1;
int totalPoints =  150; //how many points we want
/* No need to change any other parameters */


BLEUart bleuart;
bool startpro = 0;
const float resolution = 0.0008836156242;
const float analogCon = 78.4;
bool atBase = false;
int infreqStep = 0; // this is for the frequency sweep
int freqStep;
uint8_t gainArr [7] = {TIA_2P75K, TIA_3P5K, TIA_7K, TIA_14K, TIA_35K, TIA_120K,
TIA_350K};
uint8_t gainIndex = 6;
int initalFreq = 1000000;
int infreqKept = 4; //length of freq set
int freq;
int freqKept;
uint8_t RefSet = REF_SOURCE_INT;
int raw;
int varyVoltage = 236;
int phase = 0;
float countPoints = 0;
int voltammStart = 0;
uint8_t bias;
float appliedVolt;
float result;
float current;
float voltage;
```

```
float biasVoltage = 0;
float biasPercent = 0;
int kclCount = 0;
float zero;
float gain;
int counter = 0;
int icounter = 0;
int sub = 0;
uint8_t TiaN;
uint8_t RefN;
uint8_t RefINT;
int newmess = 0;
LMP91000 lmp;
uint8_t buf[64];
uint8_t rec[64];
int len;
int i = 0;
int reci = 0;
int togglee = 1;
int counttt = 0;
int voltPoints = 0;


void setup(void) {
  Serial.begin(115200);
  Wire.begin();
  analogReadResolution(12);
  pinMode(MENB, OUTPUT);  //The enable to use I2C
  pinMode (sensor, INPUT); //The output from the LMP91000
  pinMode (vref, OUTPUT);
```

```
  configSettings();
  bluetoothStart();



}

void configSettings() {

  if (vrefVoltage != 0.00) {
    RefSet = REF_SOURCE_EXT;
    analogWrite(vref, vrefVoltage * analogCon);
    delay(25); // rise time delay
    vdd = vrefVoltage;
  }

  freq = initalFreq;
  freqKept = infreqKept * 1000000;
  freqStep = infreqStep;
  accuracyVolt = 3000 / accuracyVolt;



  digitalWrite(MENB, HIGH);
  delay(5);
  digitalWrite(MENB, LOW); //active low
  delay(1);
  if (autoCali == true)
    TiaSet = gainArr[gainIndex];
  lmp.change(TiaSet | RSet, RefSet | IntSet | SignSet | BiasSet, FetSet |
ModeSet);//Write inital parameters
```

```
  setGainZero();
  delay(10); //wait a tad to start
  // displayInit(); //Checks/displays if lmp91000 was configured
}

void bluetoothStart() {
  Bluefruit.autoConnLed(true);

  Bluefruit.configPrphBandwidth(BANDWIDTH_MAX);

  Bluefruit.begin();
  Bluefruit.setTxPower(4);
  Bluefruit.setName("ElectroChemical");


  // Configure and Start BLE Uart Service
  bleuart.begin();

  // Set up and start advertising
  startAdv();
}



void startAdv(void)
{
  // Advertising packet

Bluefruit.Advertising.addFlags(BLE_GAP_ADV_FLAGS_LE_ONLY_GENERAL_DISC_
MODE);
```

```
  Bluefruit.Advertising.addTxPower();

  // Include bleuart 128-bit uuid
  Bluefruit.Advertising.addService(bleuart);
  Bluefruit.ScanResponse.addName();


  Bluefruit.Advertising.restartOnDisconnect(true);
  Bluefruit.Advertising.setInterval(32, 244);    // in unit of 0.625 ms
  Bluefruit.Advertising.setFastTimeout(30);      // number of seconds in fast mode
  Bluefruit.Advertising.start(0);                // 0 = Don't stop advertising after n seconds
}



void loop(void) {

  while ( bleuart.available() )
  {
    newmess = 1;
    rec [reci] = (uint8_t) bleuart.read();
    reci++;
  }
  if (newmess == 1) {
    decoder();
    reci = 0;
  }

  if (startpro == 1) {
```

```
switch (function) {
  case 0:
    delay(delayTime);
    currentVtime();
    displayRes();
    break;
  case 1:
    voltammetry();
    break;
  case 2:
    ImpTime();
    break;
  case 3:
    FrequencyCurrent();
    break;
  case 4:
    FrequencyImpedence();
    break;
  case 5:
    delay(delayTime);
    currentVtime();
    displayResBoth();
    break;
  case 6:
    delay(freq);
    freq = freq - freqStep;
    if (freq <= 0) {
      startpro = 0;
    }
    currentVtime();
```

```
    displayResBoth();
    break;
  case 7:
    if (kclCount < (6000 / 100)) {
      delay(delayTime);
      currentVtime();
      kclCount ++;
    }
    else {
      kclCount = 0;
      result = (result - 1.32) + 1.32;
      displayConc();
    }
    break;
  default:
    break;
}

if (autoCali == true && (raw > 3700 || raw < 25) && atBase == false) {
  if (gainIndex == 0) {
    Serial.println("Chemical Concentration is to high");
    atBase = true;
  }
  else {

    gainIndex--;
    configSettings();
    Serial.print("lowering gain to: ");
    Serial.print(gain * 1000);
    Serial.println("k");
```

```
      }
      if (function == 1) {
        voltammStart = 0;
        Serial.println("Restarting Voltammetry");
      }

    }
  }
  else {
    voltammStart = 0;
    freq = initalFreq;
    gainIndex = 6;
    freqKept = infreqKept * 1000000;
  freqStep = infreqStep;
    kclCount = 0;
  }

}



 void FrequencyCurrent() {
  int freqCount;
  float freqTot = 0;
  for ( freqCount = 0; freqCount < (freqKept / freq); freqCount ++) {
    delayMicroseconds(freq);
    raw = analogRead(sensor);
    voltage = resolution * raw;
    freqTot = freqTot + ((voltage - (vdd * zero))) / gain;
```

```
  }
result = freqTot / freqCount;
displayResF();
  freqStep = freqStep + 10;
  freq = 1000000/freqStep;
  if (freqStep >= 1000) {
  startpro = 0;
  }

}

void displayResF () {

  Serial.print(1000000/freq);
  Serial.print ("\t");
  Serial.println(result);

  setupTx();
  bleuart.write( buf, len + 1 );

}



void displayRes () {
Serial.print(raw);
  Serial.print("\t");
  Serial.println(result);
  setupTx();
  bleuart.write( buf, len + 1 );
```

```
}

void displayConc() {
  Serial.println(result);
  setupTx();
  bleuart.write( buf, len + 1 );
}

void displayVoltammRes () {

  Serial.print(raw);
  Serial.print("\t");

  Serial.print(biasVoltage, 3);
  Serial.print("\t");
  Serial.println (result);

  setupTx();
  bleuart.write( buf, len + 1 );
}


void displayResBoth () {
  Serial.print(result);
  Serial.print("\t");
  if ( result < 0) {
    result = appliedVolt * -1000000 / result;
  }
  else {
    result = appliedVolt * 1000000 / result;
```

```
  }

  Serial.println(result);

  setupTx();
  bleuart.write( buf, len + 1 );
}

void setupTx() {

  String b = (String)result;
  len = b.length();
  char c[len];
  b.toCharArray(c, len + 1);

  for ( i = 0; i < len; i++) {
    buf[i] = c[i];
  }
  buf[i] = 10;
}

void currentVtime() {
  raw = analogRead(sensor);
  voltage = resolution * raw;
  result = (voltage - (vdd * zero)) / gain;


}
```

```
void FrequencyImpedence() {
  int freqCount;
 float freqTot = 0;
  for (freqCount = 0; freqCount < (freqKept / freq); freqCount ++) {
    delay(freq);
    raw = analogRead(sensor);
    voltage = resolution * raw;
    current = (voltage - (vdd * zero)) / gain;
    if ( current < 0) {
      freqTot = freqTot +(appliedVolt * -100000000 / current);
    }
    else{
      result = freqTot + (appliedVolt * 100000000 / current);
    }
  }
  result = freqTot / (100 * freqCount);
  displayResF();
  freqStep = freqStep + 10;
  freq = 1000000/freqStep;
  if (freqStep >= 1000) {
  startpro = 0;
}
}


void ImpTime() {
  delay(delayTime);
  raw = analogRead(sensor);
```

```
  voltage = resolution * raw;
  current = (voltage - (vdd * zero)) / gain;
  if ( current < 0) {
    result = appliedVolt * -1000000 / current;
  }
  else {
    result = appliedVolt * 1000000 / current;
  }

  displayRes();
}


void voltammetry() {

  if (voltammStart == 0) {
    lmp.sweep(128 | IntSet | 13);
    voltammStart = 1;
    phase = 1;
    sub = 1;
    voltPoints = 933 / totalPoints;
    varyVoltage = 236;
    biasPercent = -24;
    analogWrite(vref, varyVoltage);
    delay(500);
  }



  delay(accuracyVolt);
```

```
if (voltPoints == 0) {

  raw = analogRead(sensor);
  voltage = resolution * raw;
  vdd = varyVoltage / 78.4;
  result = (voltage - (vdd * zero)) / gain; //current
  biasVoltage = (vdd * biasPercent) / 100;
  displayVoltammRes();
  voltPoints = 933 / totalPoints;
}
else {
  voltPoints--;
}


if (phase == 1) {


  if ( varyVoltage <= 118 && sub == 1) {
    sub = 2;
    biasPercent = -12;
    lmp.sweep(128 | IntSet | 7);
    varyVoltage = 236;
  }
  else if ( varyVoltage <= 118 && sub == 2) {
    sub = 4;
    biasPercent = -6;
    lmp.sweep(128 | IntSet | 4);
    varyVoltage = 236;
  }
```

```
  else if ( varyVoltage <= 118 && sub == 4) {
    sub = 6;
    biasPercent = -4;
    lmp.sweep(128 | IntSet | 3);
    varyVoltage = 177;
  }
  else if ( varyVoltage <= 118 && sub == 6) {
    sub = 12;
    biasPercent = -2;
    lmp.sweep(128 | IntSet | 2);
    varyVoltage = 236;
  }
  else if ( varyVoltage <= 118 && sub == 12) {
    sub = 24;
    biasPercent = -1;
    lmp.sweep(128 | IntSet | 1);
    varyVoltage = 236;
  }
  else if ( varyVoltage <= 118 && sub == 24) {
    biasPercent = 0;
    lmp.sweep(128 | IntSet | 0);
    varyVoltage = 142;
    phase = 2;
  }

  varyVoltage = varyVoltage - sub;
  analogWrite(vref, varyVoltage);

}
```

```
else if ( phase == 2) {
  biasPercent = 1;
  lmp.sweep(128 | IntSet | 16 | 1);
  phase = 3;
}

else if (phase == 3) {


  if ( varyVoltage >= 235 && sub == 1) {
    biasPercent = 24;
    lmp.sweep(128 | IntSet | 16 | 13);
    phase = 4;
  }
  else if ( varyVoltage >= 236 && sub == 2) {
    sub = 1;
    biasPercent = 24;
    lmp.sweep(128 | IntSet | 16 | 13);
    varyVoltage = 118;
  }
  else if ( varyVoltage >= 236 && sub == 4) {
    sub = 2;
    biasPercent = 12;
    lmp.sweep(128 | IntSet | 16 | 7);
    varyVoltage = 118;
  }
  else if ( varyVoltage >= 177 && sub == 6) {
    sub = 4;
    biasPercent = 6;
    lmp.sweep(128 | IntSet | 16 | 4);
```

```
    varyVoltage = 118;
  }
  else if ( varyVoltage >= 236 && sub == 12) {
    sub = 6;
    biasPercent = 4;
    lmp.sweep(128 | IntSet | 16 | 3);
    varyVoltage = 118;
  }
  else if ( varyVoltage >= 236 && sub == 24) {
    sub = 12;
    biasPercent = 2;
    lmp.sweep(128 | IntSet | 16 | 2);
    varyVoltage = 118;
  }

  varyVoltage = varyVoltage + sub;
  analogWrite(vref, varyVoltage);
}


else  if (phase == 4) {

  if ( varyVoltage <= 118 && sub == 1) {
    sub = 2;
    biasPercent = 12;
    lmp.sweep(128 | IntSet | 16 | 7);
    varyVoltage = 236;
  }
  else if ( varyVoltage <= 118 && sub == 2) {
    sub = 4;
```

```
  biasPercent = 6;
  lmp.sweep(128 | IntSet | 16 | 4);
  varyVoltage = 236;
}
else if ( varyVoltage <= 118 && sub == 4) {
  sub = 6;
  biasPercent = 4;
  lmp.sweep(128 | IntSet | 16 | 3);
  varyVoltage = 177;
}
else if ( varyVoltage <= 118 && sub == 6) {
  sub = 12;
  biasPercent = 2;
  lmp.sweep(128 | IntSet | 16 | 2);
  varyVoltage = 236;
}
else if ( varyVoltage <= 118 && sub == 12) {
  sub = 24;
  biasPercent = 1;
  lmp.sweep(128 | IntSet | 16 | 1);
  varyVoltage = 236;
}
else if ( varyVoltage <= 118 && sub == 24) {
  biasPercent = 0;
  lmp.sweep(128 | IntSet | 0);
  varyVoltage = 142;
  phase = 5;
}

varyVoltage = varyVoltage - sub;
```

```
  analogWrite(vref, varyVoltage);

}
else if ( phase == 5) {
  biasPercent = -1;
  lmp.sweep(128 | IntSet | 1);
  phase = 6;

}

else if (phase == 6) {


  if ( varyVoltage >= 236 && sub == 1) {
    biasPercent = 0;

    RefSet = REF_SOURCE_INT;
    vdd = 3.3;
    if (vrefVoltage != 0.00) {
      RefSet = REF_SOURCE_EXT;
      vdd = vrefVoltage;
    }
    lmp.sweep(RefSet | IntSet | SignSet | BiasSet);
    varyVoltage = (vrefVoltage * analogCon) - 1;
    startpro = 0;
  }
  else if ( varyVoltage >= 236 && sub == 2) {
    sub = 1;
    biasPercent = -24;
    lmp.sweep(128 | IntSet  | 13);
```

```
    varyVoltage = 118;
  }
  else if ( varyVoltage >= 236 && sub == 4) {
    sub = 2;
    biasPercent = -12;
    lmp.sweep(128 | IntSet  | 7);
    varyVoltage = 118;
  }
  else if ( varyVoltage >= 177 && sub == 6) {
    sub = 4;
    biasPercent = -6;
    lmp.sweep(128 | IntSet  | 4);
    varyVoltage = 118;
  }
  else if ( varyVoltage >= 236 && sub == 12) {
    sub = 6;
    biasPercent = -4;
    lmp.sweep(128 | IntSet  | 3);
    varyVoltage = 118;
  }
  else if ( varyVoltage >= 236 && sub == 24) {
    sub = 12;
    biasPercent = -2;
    lmp.sweep(128 | IntSet  | 2);
    varyVoltage = 118;
  }

  varyVoltage = varyVoltage + sub;
  analogWrite(vref, varyVoltage);
}
```

```
}

void setGainZero() {
  TiaN = TiaSet;
  switch (TiaN) {
    case 4:
      gain = 0.00275;
      break;
    case 8:
      gain = 0.0035;
      break;
    case 12:
      gain = 0.007;
      break;
    case 16:
      gain = 0.014;
      break;
    case 20:
      gain = 0.035;
      break;
    case 24:
      gain = 0.12;
      break;
    case 28:
      gain = 0.35;
      break;
    default:
      gain = 0;
      break;
  }
```

```
RefINT = IntSet | RefSet;
switch (IntSet) {
  case 0:
    zero = 0.2;
    break;
  case 32:
    zero = 0.5;
    break;
  case 64:
    zero = 0.67;
    break;
  default:
    zero = 0;
    break;
}

if (RefSet == 0) {
  switch (BiasSet) {
    case 0:
      appliedVolt = vdd * 0;
      break;
    case 1:
      appliedVolt = vdd * 0.01;
      break;
    case 2:
      appliedVolt = vdd * 0.02;
      break;
    case 3:
      appliedVolt = vdd * 0.04;
```

```
  break;
case 4:
  appliedVolt = vdd * 0.06;
  break;
case 5:
  appliedVolt = vdd * 0.08;
  break;
case 6:
  appliedVolt = vdd * 0.10;
  break;
case 7:
  appliedVolt = vdd * 0.12;
  break;
case 8:
  appliedVolt = vdd * 0.14;
  break;
case 9:
  appliedVolt = vdd * 0.16;
  break;
case 10:
  appliedVolt = vdd * 0.18;
  break;
case 11:
  appliedVolt = vdd * 0.20;
  break;
case 12:
  appliedVolt = vdd * 0.22;
  break;
case 13:
  appliedVolt = vdd * 0.24;
```

```
      break;
  }


}
else {
  switch (BiasSet) {
    case 0:
      appliedVolt = vrefVoltage * 0;
      break;
    case 1:
      appliedVolt = vrefVoltage * 0.01;
      break;
    case 2:
      appliedVolt = vrefVoltage * 0.02;
      break;
    case 3:
      appliedVolt = vrefVoltage * 0.04;
      break;
    case 4:
      appliedVolt = vrefVoltage * 0.06;
      break;
    case 5:
      appliedVolt = vrefVoltage * 0.08;
      break;
    case 6:
      appliedVolt = vrefVoltage * 0.10;
      break;
    case 7:
      appliedVolt = vrefVoltage * 0.12;
```

```
        break;
      case 8:
        appliedVolt = vrefVoltage * 0.14;
        break;
      case 9:
        appliedVolt = vrefVoltage * 0.16;
        break;
      case 10:
        appliedVolt = vrefVoltage * 0.18;
        break;
      case 11:
        appliedVolt = vrefVoltage * 0.20;
        break;
      case 12:
        appliedVolt = vrefVoltage * 0.22;
        break;
      case 13:
        appliedVolt = vrefVoltage * 0.24;
        break;
    }

  }
}


void displayInit() {
  Serial.println("Initial setting for the LMP91000");
  Serial.print("TIA: ");
  Serial.println(lmp.read(TIACTRL), HEX);
  Serial.print("Reference: ");
```

```
  Serial.println(lmp.read(REFCTRL), HEX);
  Serial.print("Mode: ");
  Serial.println(lmp.read(MODECTRL), HEX);
}


void connect_callback(uint16_t conn_handle)
{
  BLEConnection* connection = Bluefruit.Connection(conn_handle);
  char central_name[32] = { 0 };
  connection->getPeerName(central_name, sizeof(central_name));

  Serial.print("Connected to ");
  Serial.println(central_name);
}

void disconnect_callback(uint16_t conn_handle, uint8_t reason)
{
  (void) conn_handle;
  (void) reason;

  Serial.println();
  Serial.println("Disconnected");
}

void decoder() {
  /* debug purpose
    for ( int k = 0; k < reci -1 ; k++){
    Serial.write(rec[k]);
    }
```

```
  Serial.println();
*/
newmess = 0;
switch (rec[0]) {
  case 'a'://TIA
    TiaSet = (rec[1] & 0xf) * 100 + (rec[2] & 0xf) * 10 + (rec[3] & 0xf);
    Serial.println("Gain set");
    break;
  case 'b'://Rload
    RSet = (rec[1] & 0xf) * 100 + (rec[2] & 0xf) * 10 + (rec[3] & 0xf);
    Serial.println("Rload set");
    break;
  case 'c': //Ref source
    RefSet = (rec[1] & 0xf) * 100 + (rec[2] & 0xf) * 10 + (rec[3] & 0xf);
    Serial.println("Ref source set");
    break;
  case 'd': //internal zero
    IntSet = (rec[1] & 0xf) * 100 + (rec[2] & 0xf) * 10 + (rec[3] & 0xf);
    Serial.println("Internal zero set");
    break;
  case 'e': //bias sign
    SignSet = (rec[1] & 0xf) * 100 + (rec[2] & 0xf) * 10 + (rec[3] & 0xf);
    Serial.println("Bias sign set");
    break;
  case 'f': //bias percent
    BiasSet = (rec[1] & 0xf) * 100 + (rec[2] & 0xf) * 10 + (rec[3] & 0xf);
    Serial.println("Bias percent set");
    break;
  case 'g': //fet change
    FetSet = (rec[1] & 0xf) * 100 + (rec[2] & 0xf) * 10 + (rec[3] & 0xf);
```

```
      Serial.println("Fet set");
      break;
    case 'h': //mode control
      ModeSet = (rec[1] & 0xf) * 100 + (rec[2] & 0xf) * 10 + (rec[3] & 0xf);
      Serial.println("Mode set");
      break;
    case 'i': //function
      function = (rec[1] & 0xf) * 10 + (rec[2] & 0xf);
      Serial.println("Function Set");
      break;
    case 'j': // mV/s for voltammerty
      accuracyVolt  = (rec[1] & 0xf) * 1000 + (rec[2] & 0xf) * 100 + (rec[3] & 0xf) * 10 +
(rec[4] & 0xf);
      Serial.println("Delay for Volt set");
      break;
    case 'k': //delay for current vs time
      delayTime = (rec[1] & 0xf) * 1000 + (rec[2] & 0xf) * 100 + (rec[3] & 0xf) * 10 + (rec[4]
& 0xf);
      Serial.println("Delay for current sample set");
      break;
    case 'l': //vref voltage
      vrefVoltage = (rec[1] & 0xf)  + (rec[3] & 0xf) * 0.1 + (rec[4] & 0xf) * 0.01;
      Serial.println("Voltage ref set");
      break;
    case 'm': //vdd
      vdd = (rec[1] & 0xf)  + (rec[3] & 0xf) * 0.1 + (rec[4] & 0xf) * 0.01;
      Serial.println("VDD set");
      break;
    case 'n': //Congfig everything
      configSettings();
```

```
  Serial.println("Reconfigured");
  break;
case 'o': //Start/Stop
  startpro =  (rec[1] & 0xf);
  //Serial.println("Start/Stop");
  break;
case 'p': //auto calibrate
  autoCali = (rec[1] & 0xf);
  Serial.println("AutoCali Toggle");
  break;
case 'q': //read lmp
  displayInit();
  break;}}
```